*Proceedings of the*
*Annual Stability Conference*
*Structural Stability Research Council*
*St. Louis, Missouri, April 16-20, 2013*

# Towards a More Rational DSM Design Approach for Angle Columns

P.B. Dinis[1], D. Camotim[1], A. Landesmann[2]

**Abstract**

This paper deals with the development of novel procedures for the design of fixed-ended and pin-ended equal-leg angle columns with short-to-intermediate lengths, *i.e.*, those buckling in flexural-torsional modes. Initially, numerical results concerning the buckling and post-buckling behavior of the above angle columns are presented, (i) highlighting the main differences between the fixed-ended and pin-ended column responses, and (ii) evidencing the need for specific design procedures. Then, the paper gathers a large column ultimate strength data bank that includes (i) experimental values, collected from the available literature, and (ii) numerical values, obtained from ABAQUS shell finite element analyses. The set of experimental results collected comprises *41* fixed-ended and *35* pin-ended columns, and the numerical results obtained concern *92* fixed-ended and *64* pin-ended columns – various cross-section dimensions, lengths and yield stresses are considered. Next, after reviewing the available methods to estimate the ultimate strength of angle columns, the paper develops new design approaches for fixed-ended and pin-ended columns, based on the Direct Strength Method (DSM) – the mechanical reasoning behind the procedures proposed, which include the use of genuine flexural-torsional strength curves, is also provided. Finally, the paper closes with the assessment of the ultimate strength predictions yielded by the proposed DSM design procedures, through their comparison with the assembled experimental and numerical failure loads – it is shown that both the quality and reliability of these predictions are very good and slightly higher than those exhibited by all the available design methods for angle columns.

## 1. Introduction

Thin-walled angle columns are known to possess no primary warping resistance (the cross-section warping constant stems exclusively from secondary warping), which implies an extremely low torsional stiffness and, therefore, a high susceptibility to instability phenomena involving torsion, namely flexural-torsional buckling (equal-leg angles are singly symmetric cross-section). Since the flexural-torsional deformations exhibited by equal-leg angle columns with short-to-intermediate lengths are very similar (akin) to local deformations, these members have been said to fail in "local-global interactive modes", which explains why most of the existing methods for their design are based on local strength concepts/curves. Since column flexural-torsional (global) and local buckling are commonly associated with markedly different post-critical behaviors (strength reserves), the definition of a rational (structurally well founded) design model/procedure to provide accurate ultimate strength estimates for thin-walled equal-leg angle columns must necessarily involve flexural-torsional strength concepts/curves (instead of local ones).

[1] Civil Engineering Department, ICIST, Instituto Superior Técnico, Technical University of Lisbon, Portugal. <dinis; dcamotim@civil.ist.utl.pt>
[2] Civil Engineering Program, COPPE, Federal University of Rio de Janeiro, Brazil. <alandes@coc.ufrj.br>

The post-buckling behavior, strength and design of angle columns has attracted the attention of several researchers in the past (*e.g.*, Kitipornchai & Chan 1987, Kitipornchai *et al.* 1990, Popovic *et al.* 1999, Young 2004, Ellobody & Young 2005, Rasmussen 2005,2006, Chodraui *et al.* 2006, Maia *et al.* 2008, Shifferaw & Schafer 2011, and Mesacasa Jr. 2012). Nevertheless, numerical simulations recently carried out by the authors (Dinis & Camotim 2011, Dinis *et al.* 2012), concerning pin-ended (but with end-section warping prevented) and fixed-ended short-to-intermediate equal-leg angle columns, shed new light on key (and somewhat surprising) mechanical aspects related with the structural response of such members, namely the fact that it is strongly influenced by the interaction between two global buckling modes (one involving major-axis flexure and torsion, and the other minor-axis flexure only)[3]. They also showed that a single design approach cannot handle adequately both pin-ended and fixed-ended angle columns – this is because, due to the effective centoid shift (*e.g.*, Young & Rasmussen 1999), the mode interaction effects are much more relevant in the former case. These findings led Dinis *et al.* (2010a, 2011) and Silvestre *et al.* (2013) to propose different design approaches for pin-ended and fixed-ended columns, both based on the Direct Strength Method (DSM – *e.g.*, Schafer 2008), which combine (i) the experimentally-based global design curve proposed by Young (2004) with (ii) either the current DSM local strength curve (fixed-ended columns) or an empirically determined lower "local" design curve (pin-ended columns). Although these DSM-based design approaches were shown (i) to provide efficient (accurate and reliable) estimates of the available pin-ended and fixed-ended experimental and numerical failure loads, and (ii) to outperform all their predecessors, they exhibit one non-negligible drawback: the lack of an underlying rational structural model. This is mainly because they do not take into account explicitly the fact that the column behavior and failure are governed by the interaction between minor-axis flexural and major-axis flexural-torsional (instead of local) buckling effects, which are markedly different for pin-ended and fixed-ended equal-leg columns (Dinis *et al.* 2012).

The aim of this work is to overcome the drawback mentioned in the previous paragraph, by contributing towards the development/proposal of more rational DSM-based design approaches for pin-ended and fixed-ended equal-leg angle columns. The key contribution consists of retaining the current DSM global strength curve, while replacing its local counterpart by a set of genuine flexural-torsional ones that are specifically developed for equal-leg angle columns and, therefore, account for the structural peculiarity of this cross-section shape – note that it is formed by just two outstands, which renders the mode interaction effects remarkably relevant (particularly in the pin-ended columns, due to the effective centroid shift). Initially, numerical results concerning the angle column buckling and post-buckling behavior are presented, (i) highlighting the differences between the fixed-ended and pin-ended column responses, and (ii) evidencing the need for specific design procedures. Then, the paper gathers a large column failure load data bank that includes (i) *76* experimental values (*41* fixed and *35* pinned specimens), collected from the available literature, and (ii) *156* numerical values (*92* fixed and *64* pinned columns), yielded by ABAQUS shell finite element analyses (SFEA) – various cross-section dimensions, lengths and yield stresses are considered. Then, after reviewing the existing methods to estimate the ultimate strength of angle columns, the paper presents the development of the aforementioned new DSM-based design approaches for fixed-ended and pin-ended columns, including the mechanical reasoning behind the procedures proposed. Finally, the paper closes with the assessment of the ultimate strength predictions provided by the novel DSM design procedures, through their comparison with the assembled failure load data bank – both the quality and reliability of these predictions are shown to be very quite good and higher than those exhibited by all the available design methods for angle columns (including those proposed by Silvestre *et al.* 2013).

[3] This interaction was very recently investigated in some detail by Mesacasa Jr. *et al.* (2012).

## 2. Buckling and Post-Buckling Behavior

The main results obtained in recent investigations on the buckling, post-buckling and ultimate strength behavior of thin-walled steel ($E=210GPa$ and $\nu=0.3$) angle columns (Dinis *et al.* 2010a,b, 2011, 2012, Dinis & Camotim 2011). The columns analyzed exhibit (i) pinned (but with the secondary warping prevented) and fixed end sections, (ii) equal legs ($70\times70$ *mm* and $t=1.2mm$ – the effect of rounded corners is disregarded) and (iii) short-to-intermediate lengths. Almost all the numerical results were obtained through ABAQUS (Simulia 2008) shell finite element analyses, (i) adopting column discretizations into fine 4-node isoparametric element meshes (length-to-width ratio close to *1*) and (ii) modeling the column supports by ($ii_1$) fully attaching the member end sections to rigid end-plates (thus ensuring the secondary warping and local displacement/rotation restraints) and ($ii_2$) preventing both the major and minor-axis flexural rotations (fixed supports – F condition) or only the major-axis flexural rotations (pinned supports with cylindrical hinge – P condition[4]) – the torsional rotations are prevented in both cases. However, in order to characterize and distinguish between local and global buckling of angle columns, GBT analyses are also performed using the code GBTUL (Bebiano *et al.* 2008a,b).

### *2.1 Buckling Behavior*

The curves shown in Fig. 1(a) provide the variation of $P_{cr}$ (critical load, obtained from ABAQUS SFEA) with the length $L$ (logarithmic scale), both for F and P columns. This figure also depicts single half-wave buckling loads ($P_{b.1}$) yielded by GBT analyses including *7* deformation modes: *4* global (**1**-**4**) and *3* local (**5**-**7**). As for Fig. 1(b), it displays the GBT modal participation diagrams for the F and P columns – they provide the contributions of each GBT deformation mode to the column single half-wave buckling modes (Dinis *et al.* 2010b). Finally, Fig. 1(c) shows the buckling mode shapes of the P columns with $L=100, 364, 1000\,cm$, as well as the in-plane shapes of the first *6* deformation modes (axial extension excluded). These buckling results prompt the following remarks:

(i) For the entire length range, the column critical buckling modes involve only participations from deformation modes **2**, **3**, **4** and **6**.

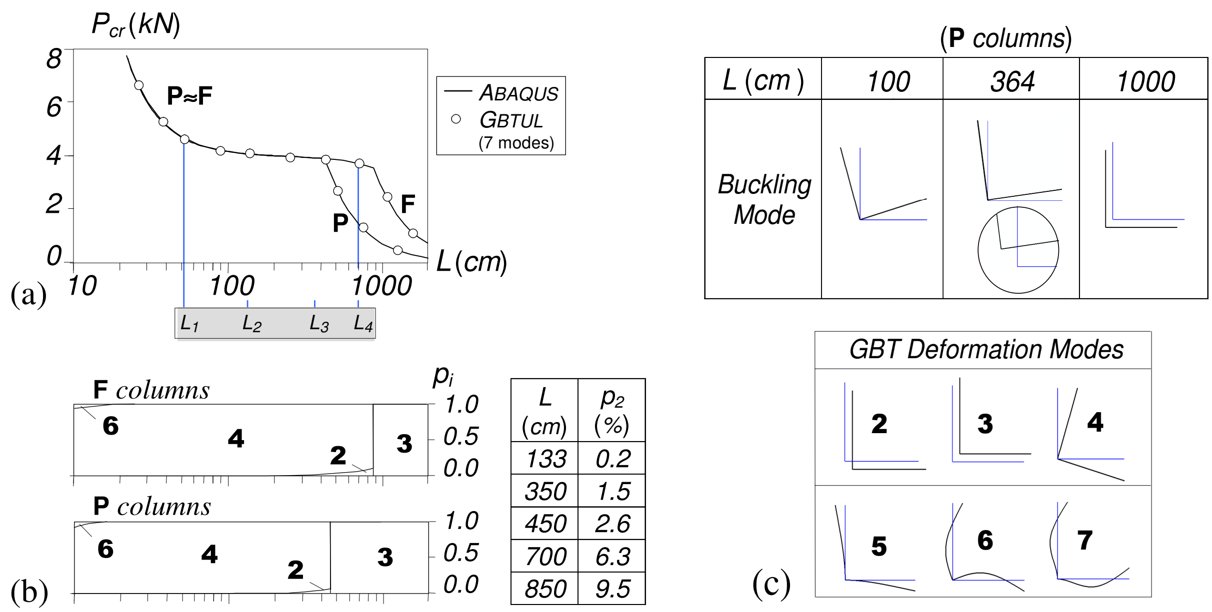


| L (cm) | $p_2$ (%) |
|---|---|
| 133 | 0.2 |
| 350 | 1.5 |
| 450 | 2.6 |
| 700 | 6.3 |
| 850 | 9.5 |

Figure 1: (a) $P_{cr}$ vs. $L$ curves and (b) GBT modal participation diagrams (F and P columns), including a table with a few $p_2$ values, and (c) in-plane shapes of *3* buckling modes and first *6* GBT deformations modes (P columns)

---

[4] These are the end support conditions adopted in the “pin-ended angle column experimental tests” reported in the literature.

(ii) Due to the cross-section single symmetry (with respect to the major-axis) all the short-to-intermediate columns buckle in flexural-torsional modes, combining participations from deformation modes **4** (torsion) and **2** (major-axis flexure), which correspond to fairly uniform critical loads defining almost horizontal "plateaus" in the $P_{cr}$ vs. $L$ curves. The participations of modes **2** and **4** vary continuously with the column length. The former is virtually imperceptible for the shorter columns and only becomes visible as $L$ increases (the growth occurs at a fairly small pace) – in order to enable a quantification of the percentage participation of mode **2** in the column buckling mode ($p_{\mathbf{2}}$), the table in Fig. 1(b) shows its variation with $L$.

(iii) Both the P and F columns display similar buckling features: (iii$_1$) $P_{cr}$ decreases monotonically with $L$ and corresponds to single half-wave buckling, (iii$_2$) the GBT and ABAQUS results virtually coincide, and (iii$_3$) the torsion mode **4** plays a key role, as it participates in the critical buckling modes of all but the long columns, which exhibit pure minor-axis flexural buckling modes (only mode **3**).

(iv) Compared to the short-to-intermediate F columns, the P columns only differ in the smaller length range corresponding to the end of the "plateau", due to the *75%* drop of the minor-axis flexural buckling loads – the transition from flexural-torsional buckling to flexural buckling occurs for $L=420cm$ (P columns) and $L=890cm$ (F columns). For lengths below $L=420cm$, the P and F column local and flexural-torsional buckling loads and modes are fully identical (for the same length).

(v) The post-buckling results presented in the next subsection concern short-to-intermediate angle columns with the following lengths (see Fig. 1(a)): $L_1=53cm$, $L_2=133cm$, $L_3=364cm$ and $L_4=700cm$ – *4* F columns ($F_1$-$F_4$ – $22.1 \leq f_{cr} \leq 27.5MPa$) and *3* P columns ($P_1$-$P_3$ – $23.4 \leq f_{cr} \leq 27.5MPa$).

### *2.2 Elastic Post-Buckling Behavior*

ABAQUS SFEA are employed to investigate the elastic and elastic-plastic post-buckling behavior of F and P angle columns (i) with the lengths indicated above, (ii) containing critical-mode initial imperfections with amplitude equal to *10%* of the wall thickness $t$ (flexural-torsional shapes with mid-span torsional rotations of about $\beta_0=0.1°$ for the angle section $70{\times}70{\times}1.2mm$) and (iii) exhibiting various yield-to-critical stress ratios (Dinis *et al.* 2010a, 2011, 2012, Dinis & Camotim 2011).

Figures 2(a)-(c) show the upper parts ($P/P_{cr}>0.6$) of the $F_1$-$F_4$ column post-buckling equilibrium paths (i) $P/P_{cr}$ *vs.* $\beta$, $P/P_{cr}$ *vs.* $d_M/t$ and $P/P_{cr}$ *vs.* $d_m/t$ – $\beta$, $d_M$ and $d_m$ are the mid-span web chord rigid-body rotation and corner displacements due to major and minor-axis flexure, respectively. As for Figs. 3(a)-(b), they concern the $F_2$-$F_4$ columns and provide the longitudinal profiles of the two corner displacements at four equilibrium states (increasing $P/P_{cr}$ values) – note that (i) the horizontal coordinate is normalized to the column length ($x_3/L$) and (ii) the $d_M/t$ and $d_m/t$ scales are substantially different for the three columns (*e.g.*, the $F_4$ column values are 80 times larger than their $F_2$ column counterparts). The observation of these elastic post-buckling results prompts the following comments:

(i) All column post-buckling behaviors involve the simultaneous occurrence of cross-section torsional rotations and flexural (corner) displacements. The relative importance of the latter has strong impact on the column post-buckling response, namely on its post-critical strength reserve.

(ii) Indeed, two column "families" can be identified, according to their post-buckling behavior: (ii$_1$) those of the shorter $F_1$-$F_3$ columns (the $F_1$ and $F_2$ columns have virtually identical equilibrium paths), which are clearly stable (fairly high post-critical strengths) and exhibit very small corner displacements, and (ii$_2$) that of the longer $F_4$ column, which exhibits significant corner displacements and has a limit point, followed by a significant torsional rotation reversal (see Fig. 2(a)), due to an abrupt switch from a single half-wave to three half-waves soon after the peak load is reached (Dinis & Camotim 2011, Dinis *et al.* 2012).

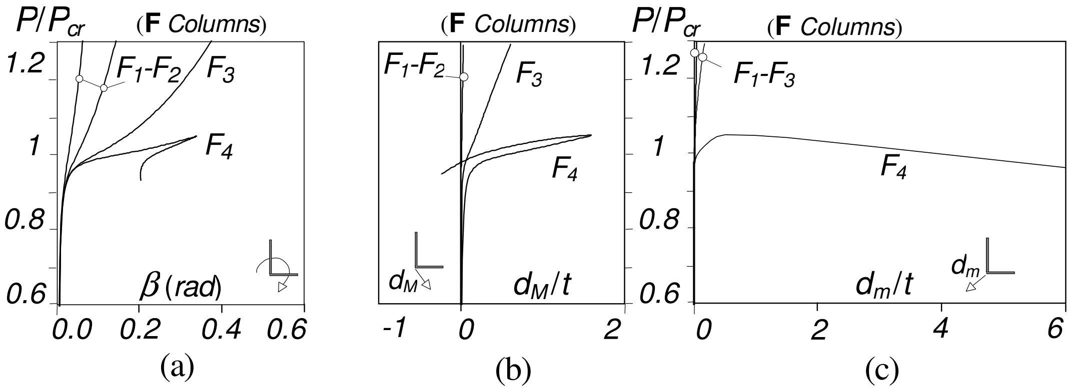


Figure 2: $F_1$-$F_4$ column (a) $P/P_{cr}$ *vs.* $\beta$, (b) $P/P_{cr}$ *vs.* $d_M/t$ and (c) $P/P_{cr}$ *vs.* $d_m/t$ equilibrium paths

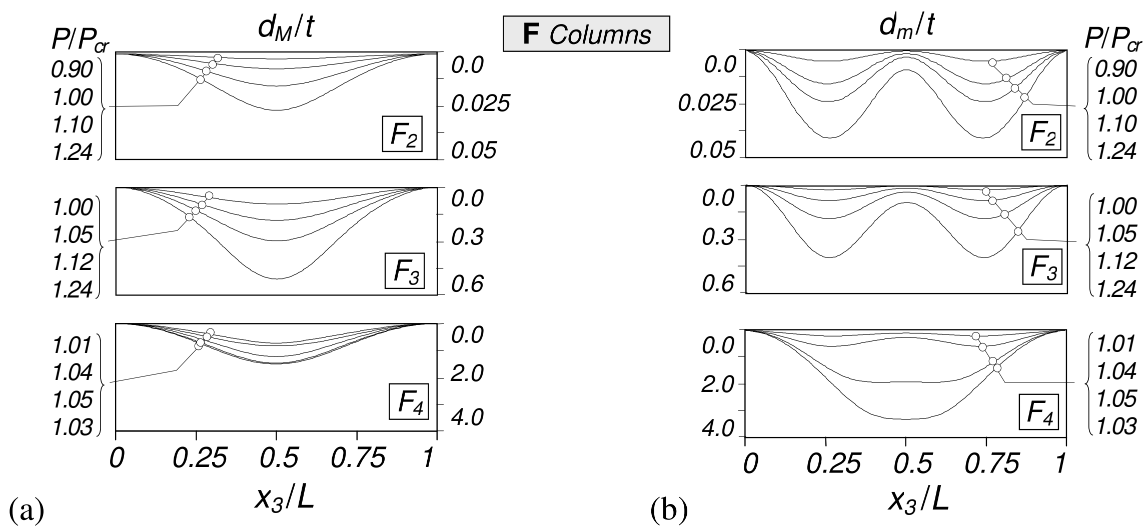


Figure 3: $F_2$-$F_4$ column (a) $d_M/t$ and (b) $d_m/t$ longitudinal profiles

(iii) Since major-axis flexure participates in the column critical buckling modes (see the participation of deformation mode **2** in Fig. 1(b)) and, therefore, incorporates the corresponding initial geometrical imperfections, it is not surprising that (iii$_1$) the $d_M$ values progressively grow with the applied load and (iii$_2$) their longitudinal profiles exhibit the typical F column critical buckling mode shape: one inner half-wave and two outer "quarter-waves" (to ensure null end slopes).

(iv) The emergence of minor-axis flexure ($d_m$ displacements), which does not participate in the column critical buckling modes and exhibits longitudinal profiles with three inner half-waves (and two outer "quarter-waves" to ensure null end slopes), stems from the longitudinal variation of the torsional rotations. These rotations cause non-linear cross-section mid-line longitudinal stress distributions that vary along the column axis according to a "three half-wave" pattern, leading to effective centroid shifts (towards the cross-section corner) that follow that same longitudinal pattern (Stowell 1951, Dinis & Camotim 2011, Dinis *et al.* 2012). These effective centroid shifts are responsible for the (positive) minor-axis flexural displacements that have some impact on the F angle column response. In the longer ($F_4$) column, this impact is overshadowed by the occurrence of fairly strong interaction with flexural buckling. Indeed, for this column length, the flexural-torsional and flexural buckling loads are fairly close and become even closer due to the axial stiffness reduction associated with the flexural-torsional post-buckling behavior.

(v) Due to the relevance of the corner displacements (mostly the $d_m$ ones), the behavior of F equal-leg angle columns can not be viewed as the "sum" of two fixed-ended (longitudinally) pinned-free (transversally) long plates, unlike it would be tempting to anticipate. In particular, the cross-section longitudinal normal stress distributions become far from parabolic as post-buckling progresses. Recently, the authors (Dinis *et al.* 2010b, 2012) showed that preventing the corner displacements makes it possible to recover the pinned-free long plate post-buckling behavior. In the case of the (long) $F_4$ column, the post-buckling behavior is significantly altered – it becomes clearly stable (no limit point) and the normal stress distributions (not shown here) change drastically, exhibiting a parabolic shape with the higher value at the pinned edge (*i.e.*, in line with the general belief).

Next, it is investigated how releasing the end sections minor-axis flexural rotations affects the post-buckling behavior of angle columns with short-to-intermediate lengths. Figs. 4(a)-(c) show the upper parts of the $P_1$-$P_3$ column post-buckling equilibrium paths $P/P_{cr}$ *vs.* $\beta$, $P/P_{cr}$ *vs.* $d_M/t$ and $P/P_{cr}$ *vs.* $d_m/t$, while Figs. 5(a)-(b) display the $P_2$-$P_3$ column $d_M/t$ and $d_m/t$ longitudinal profiles at three equilibrium states (increasing $P/P_{cr}$ values). The observation of these P column post-buckling results, as well as the comparison with their F column counterparts, leads to the following conclusions:

(i) It is again possible to define two P column "families", according to their post-buckling behavior: ($i_1$) the $P_1$ column is clearly stable and exhibits minute mid-span corner displacements, and ($i_2$) the $P_2$-$P_3$ columns are barely stable, experience significant mid-span corner displacements and exhibit limit points – either abrupt and followed by a torsional rotation reversal ($P_2$ column), or smooth and without torsional rotation reversal ($P_3$ column) – the amount of corner flexural displacements plays a key role in separating the various post-buckling behaviors.

(ii) The F and P column equilibrium paths share a few common features: ($ii_1$) the $d_M$ displacements remain always very small (they grow with $L$ and their longitudinal profiles retain the typical fixed-ended critical buckling mode shape) and ($ii_2$) the rotation reversals coincide with the torsional rotation "switch" from a single to three half-waves.

(iii) However, there are some important differences between the evolutions of the $d_m/t$ longitudinal profiles in the F and P columns: while the former exhibit three inner half-waves (plus two external "quarter-waves" to ensure null end slopes), the latter apparently exhibit just a single half-wave[5]. Moreover, note that the P column $d_m$ values are significantly higher (about ten times) than their $d_M$

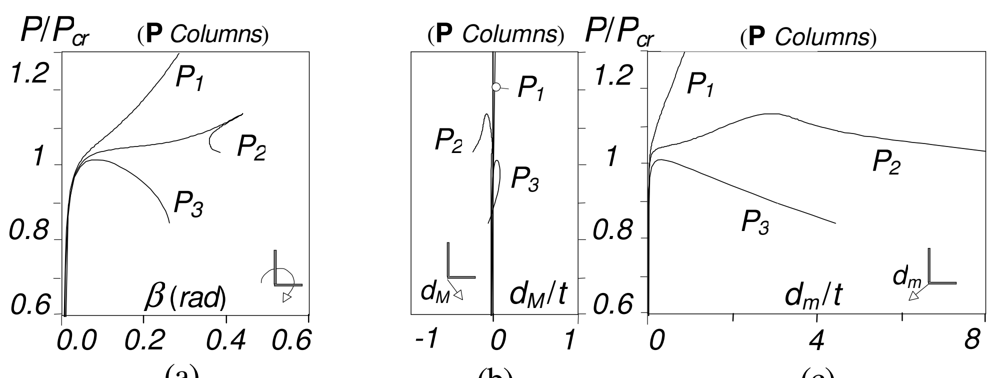


Figure 4: $P_1$-$P_3$ columns: (a) $P/P_{cr}$ *vs.* $\beta$, (b) $P/P_{cr}$ *vs.* $d_M/t$ and (c) $P/P_{cr}$ *vs.* $d_m/t$ equilibrium paths

[5] A closer look at the $d_m/t$ longitudinal profiles of the $P_2$ and $P_3$ columns reveals that the former exhibits a half-wave with a "flat" central region that decreases as the loading progresses – this does not occur in the $P_3$ column, which exhibits a "well curved" half-wave. This "flat" central region corresponds to the combination of (i) a dominant "well curved" half-wave with (ii) less relevant three half-waves – the presence of the latter is virtually imperceptible in the $P_3$ column (Dinis *et al.* 2012).

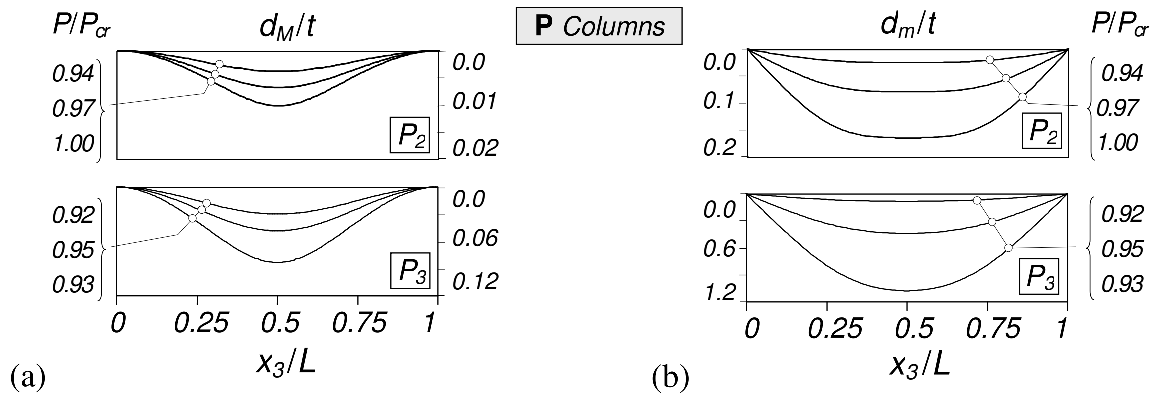


Figure 5: $P_2$-$P_3$ columns: (a) $d_M/t$ and (b) $d_m/t$ longitudinal profiles

counterparts – their magnitude are similar (and small) for F columns (before the interaction with the minor-axis flexural buckling mode takes place, of course).

(iv) The differences described in the previous item stem from the absence of the minor-axis end moments, which means that it is no longer possible to oppose the minor-axis bending caused by the "effective centroid shifts" occurring due to the cross-section normal stress redistribution (*e.g.*, Young & Rasmussen 1999). Indeed, although the mechanical reasoning behind the development of the three half-wave $d_m$ profile remains valid for the P columns (recall that the end section secondary warping and torsional rotation are still prevented), the predominance of the "well curved" (sinusoidal) half-wave component now largely overshadows it. Such predominance is even clearer in the longer columns, such as the $P_3$ one, due to the more intense interaction with minor-axis flexural buckling (closer flexural-torsional and flexural buckling loads).

*2.3 Elastic-Plastic Post-Buckling Behavior*

The elastic-plastic behavior and strength of F and P short-to-intermediate angle columns is briefly addressed now. The results presented next concern columns (i) still containing critical-mode initial imperfections with $0.1t$ amplitude and (ii) exhibiting four yield-to-critical stress ratios ($f_y/f_{cr}\approx 1.3, 2.5, 5.0$ – $f_y=30, 60, 120MPa$ and "average" $f_{cr}=24MPa$) – some unrealistically low yield stresses are considered, to cover a wide slenderness range. For comparative purposes, a few elastic results presented earlier are shown again (they correspond to $f_y=f_y/f_{cr}=\infty$).

Fig. 6(a) depicts typical shorter F column elastic-plastic equilibrium paths. It shows the upper portions ($P/P_{cr}>0.5$) of the $F_3$ column $P/P_{cr}$ *vs.* $\beta$ paths for the yield-to-critical stress ratios $f_y/f_{cr}\approx 1.3, 2.5, 5.0$ (and also the elastic path already shown in Fig. 2(a)). Fig. 6(b), on the other hand, displays three plastic strain diagrams, corresponding to equilibrium states located along the $f_y/f_{cr}\approx 2.5$ equilibrium path (as indicated in Fig. 6(a)) and including the column collapse mechanism. As for Figs. 7(a)-(b), they illustrate a typical longer F elastic-plastic post-buckling behavior. They show the upper portions of the $F_4$ column $P/P_{cr}$ *vs.* $\beta$ paths concerning four $f_y/f_{cr}$ values and also the column deformed configuration and plastic strain evolution, for $f_y/f_{cr}\approx 2.5$. The observation of all these results leads to the following remarks:

(i) While the $F_3$ columns with $f_y/f_{cr}\approx 1.3$, $2.5$ fail at the onset of yielding, their $f_y/f_{cr}\approx 5.0$ counterpart exhibits a very small elastic-plastic strength reserve. The $F_3$ column ultimate load grows visibly with $f_y$ – *e.g.*, an increase from $30$ to $120MPa$ more than doubles the load-carrying capacity.

(ii) Diagram *I* in Fig. 6(b) shows that, in the $F_3$ columns, yielding starts around the quarter and three quarter-span zones of the corner longitudinal edge, where the shear and longitudinal normal stresses, due to the torsional rotation variation, are higher (Stowell 1951, Dinis *et al.* 2012).

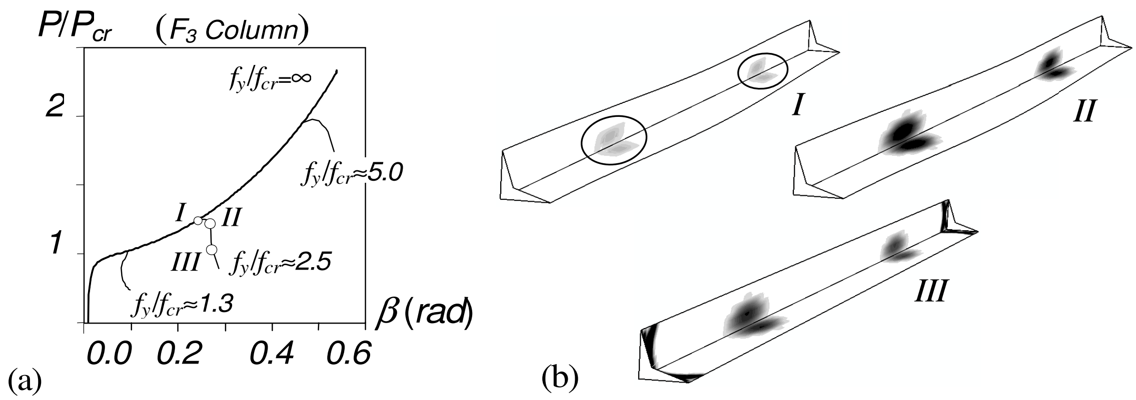


Figure 6: $F_3$ column elastic-plastic post-buckling behavior: (a) $P/P_{cr}$ *vs.* $\beta$ equilibrium paths, for $f_y/f_{cr}$≈*1.3*, *2.5*, *5.0*, and (b) plastic strain diagrams and failure mechanism, for $f_y/f_{cr}$≈*2.5*

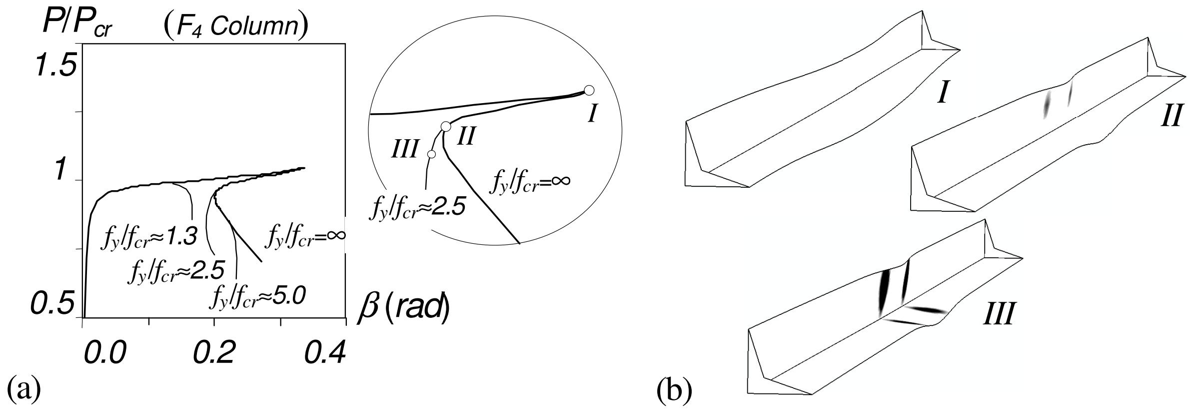


Figure 7: $F_4$ column elastic-plastic post-buckling behavior: (a) $P/P_{cr}$ *vs.* $\beta$ equilibrium paths, for $f_y/f_{cr}$≈*1.3*, *2.5*, *5.0*, and (b) plastic strain diagrams and (elastic) failure mode, for $f_y/f_{cr}$≈*2.5*

(iii) The longer $F_4$ column ultimate strength is practically insensitive to $f_y$, as the collapse is predominantly due to geometrically non-linear effects. Indeed, for $f_y/f_{cr}$≈*2.5*,*5.0* the column remains elastic up until failure, as the onset of yielding only takes place well inside the equilibrium path descending branch – it occurs in the middle of the vertical leg mid-span region, as illustrated in Fig. 7(b) (diagram II).

A similar investigation was performed for the P columns. Figs. 8(a)-(b) display (i) the upper parts ($P/P_{cr}>0.5$) of the $P/P_{cr}$ *vs.* $\beta$ paths concerning $P_2$ columns with $f_y/f_{cr}$≈*1.3*,*2.5*,*5.0*, ∞, and (ii) the plastic strain evolution and collapse mechanism of the $P_2$ column with $f_y/f_{cr}$≈*2.5*. The observation of these post-buckling results prompts the following comments:

(i) There is virtually no elastic-plastic strength reserve or ductility prior to failure – yielding starts in the middle of the vertical leg quarter-span and three quarter-span (see diagram *I* in Fig. 8(b)) and precipitates the column collapse.

(ii) There is a rather small variation of the column ultimate load with the yield stress – *e.g.*, a rise from *30* to *120MPa* entails a small failure load increase (only *9.4%*). Moreover, there is no benefit in increasing the yield stress beyond five times $f_{cr}$, since for $f_y/f_{cr}$≈*5.0* the collapse occurs, abruptly, in the elastic range (the $f_y/f_{cr}$≈*5.0* and $f_y/f_{cr}$≈∞ curves share the same limit point).

(iii) The above $P_2$ column post-buckling behavior features are also exhibited, to an even larger extent, by the longer P columns, such as the $P_3$ one – recall its elastic post-buckling equilibrium paths, shown in Figs. 4(a)-(c), which display smooth limit points for $P/P_{cr}$≈*1.0*.

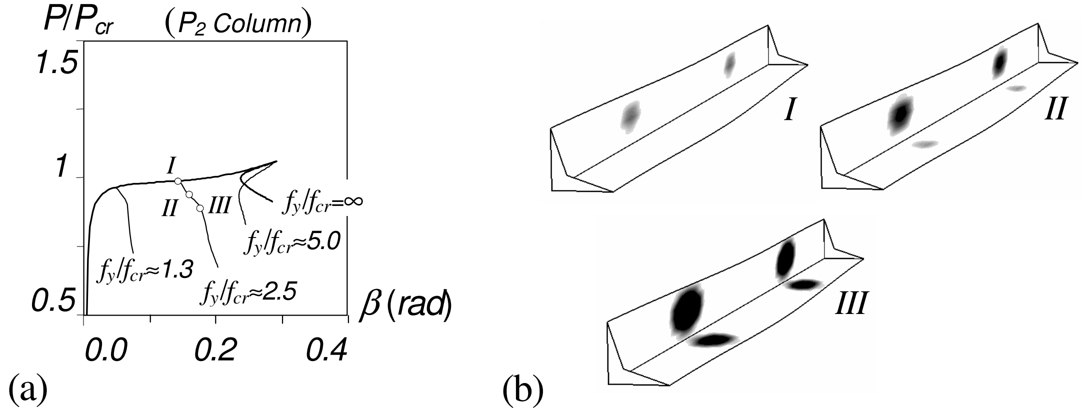


Figure 8: $P_2$ column elastic-plastic post-buckling behavior: (a) $P/P_{cr}$ *vs.* $\beta$ equilibrium paths, for $f_y/f_{cr}\approx 1.3$, $2.5$, $5.0$, and (b) plastic strain diagrams and failure mode, for $f_y/f_{cr}\approx 2.5$

The markedly different elastic and elastic-plastic post-buckling behaviors displayed by the F and P short-to-intermediate equal-leg angle columns implies that there is a significant discrepancy between their ultimate strengths $P_u$ associated with a given yield stress. Since all these columns have virtually identical critical stresses, thus sharing a common critical slenderness $\lambda=(P_y/P_{cr})^{0.5}$, their $P_u/P_y$ values may exhibit a high "vertical dispersion" with respect to $\lambda$ – this behavioral feature must be adequately taken into account by an efficient design procedure for equal-leg angle columns.

## 3. Failure Load Data: Test Results and Numerical Simulations

Following the findings reported by Dinis *et al.* (2010a, 2011, 2012) and Dinis & Camotim (2011), which were summarized above, Silvestre *et al.* (2013) decided to assess the performance of the then existing design rules for cold-formed steel equal-leg angle columns with short-to-intermediate lengths. This task required the assembly a fairly large column ultimate strength data bank, comprising (i) experimental failure loads reported in literature and (ii) numerical failure loads determined by means of ABAQUS SFEA (employing the model developed earlier, also used to obtain the results presented in the previous section).

The experimental failure loads concern (i) *41* fixed-ended columns, tested by Popovic *et al.* (1999), Young (2004) and Mesacasa Jr. (2012)[6], and (ii) *35* pin-ended columns (with cylindrical supports), tested by Wilhoite *et al.* (1984), Popovic *et al.* (1999), Chodraui *et al.* (2006) and Maia *et al.* (2008). The specimen cross-section geometries, lengths $L$, yield stresses $f_y$ and ultimate stresses $f_u$ are given in Annex A (F columns) and Annex B (P columns). Detailed accounts of these experimental investigations can be found in the above publications – see also the overview provided by Silvestre *et al.* (2013).

The numerical (SFEA) failure loads concern (i) *92* fixed-ended and (ii) *64* pin-ended columns, exhibiting (i) three cross-section dimensions (*70×1.2mm, 50×1.2mm* and *50×2.6mm*), (ii) lengths selected to ensure critical flexural-torsional modes buckling (*i.e.*, all the columns fall within the $P_{cr}$ vs. $L$ curve "horizontal plateaus" shown in Fig. 1(a)) and (iii) yield stresses chosen to enable covering a wide critical slenderness range. The column cross-section geometries, selected lengths $L$, adopted yield stresses $f_y$ and obtained ultimate stresses $f_u$ are given in Annex C (F columns) and Annex D (P columns). It is worth

[6] Four tests reported by Maia *et al.* (2008) were excluded from this study, since the ultimate strengths reported are much lower than the numerical results obtained by the same authors, adopting fair-to-high torsional initial imperfections (*0.64t* and *1.55t*). In our opinion, these fixed-ended columns contained abnormally large initial imperfections and/or load eccentricities (possibly caused by the procedure adopted to ensure the column end section fixity).

noting that all the F column and part of the P column results shown here were already reported by Silvestre *et al.* (2013) – the remaining ones, determined in the context of this investigations, concern P columns with the following cross-section dimensions and lengths: (i) $50\times2.6mm$ and $L=750,950mm$, and (ii) $50\times1.2mm$ and $L=750,950,1500,2000mm$. In all the analyses, the steel material behavior was modeled as elastic-perfectly plastic ($E=210GPa$, $\nu=0.3$) and both the residual stresses and rounded corner effects are disregarded. Preliminary numerical studies showed that the combined influence of strain hardening, residual stresses and rounded corner effects has little impact on the angle column failure loads (all differences below $3\%$), which is in line with the findings reported by other authors, namely Ellobody & Young (2005) and Shi *et al.* (2009). As mentioned earlier, the yield stresses $f_y$ were selected to cover a wide critical slenderness range, which implied considering a few unrealistic (small) values – the yield stress values adopted were (i) $30,60,120,235,400,500MPa$ ($70\times1.2mm$ columns), and (ii) $120,235,400,500MPa$ ($50\times1.2mm$ and $50\times2.6mm$ columns).

Following the behavior observed in the experimentally tested columns, namely the length-dependency of the imperfection-sensitivity, a preliminary study was carried out to identify the most detrimental imperfection shape – critical flexural-torsional and/or minor-axis flexural shape. Although the column with shorter lengths (left and central zones of the $P_{cr}(L)$ curve horizontal plateaus) were found to be virtually insensitive to the minor-axis flexural imperfections (only the flexural-torsional imperfections are relevant)[7], it was decided to determine, for all the F and P columns analyzed, failure loads stemming from the simultaneous presence of flexural-torsional and minor-axis flexural initial geometrical imperfections – the columns contained initial imperfections combining (i) a critical flexural-torsional component, with amplitude equal to $10\%$ of the wall thickness $t$, and (ii) a non-critical minor-axis flexural component, with amplitude equal to $L/750$ (F columns) or $L/1000$ (P columns)[8] – values in line with the measurements reported for the column specimens tested by Young (2004) and Popovic *et al.* (1999), respectively.

## 4. Review of the Available Design Methods

Regarding the available design methods for concentrically loaded equal-leg angle columns, the earlier AISI (1996) and NAS (AISI 2001) specifications prescribed ultimate strength estimates of the form

$$P_n = A_e \cdot f_n \quad , \quad (1)$$

where $A_e$ is the angle effective cross-section area and $f_n$ is the column global strength, given by

$$f_n = \begin{cases} f_y\left(0.658^{\lambda_c^2}\right) & if \quad \lambda_c \le 1.5 \\ f_y\left(\dfrac{0.877}{\lambda_c^2}\right) & if \quad \lambda_c > 1.5 \end{cases} \qquad \text{with} \qquad \lambda_c = \sqrt{\frac{f_y}{f_{cre}}} \quad , \quad (2)$$

where $f_y$ is the yield stress, $f_{cre}$ is the critical global buckling stress and $\lambda_c$ is the global slenderness. Since (i) $f_n$ is based on the minimum between the flexural-torsional (major-axis) and flexural (minor-axis) buckling stresses, and (ii) $A_e$ is based on the local (or torsional) buckling stress, Popovic *et al.* (2001) showed that the above procedure led to overly conservative $P_n$ values, because the torsional buckling stress comes into play twice (through $f_n$ and $A_e$). In order to achieve more accurate (but still safe) ultimate strength predictions, these authors proposed a modification: to base (i) $f_n$ on the flexural (minor-axis)

[7] A detailed investigation on the imperfection-sensitivity, associated with the simultaneous presence of flexural-torsional and minor-axis flexural initial imperfections, of equal-leg angle columns was very recently reported by Mesacasa Jr. *et al.* (2013).

[8] The initial $d_m$ values always "point" towards the cross-section corner, thus reinforcing the effective centroid shift effects.

buckling stress alone, and (ii) $A_e$ on the local (torsional) buckling stress. Later, Young (2004) tested fixed-ended angle columns and showed that the modified AISI/NAS estimates were (i) still conservative for stocky columns and (ii) unsafe for slender columns. In order to improve the quality of the estimates, he proposed the use of a modified global strength curve, given by

$$f_{ne} = \begin{cases} f_y \left(0.5^{\lambda_c^2}\right) & if \quad \lambda_c \leq 1.4 \\ f_y \left(\dfrac{0.5}{\lambda_c^2}\right) & if \quad \lambda_c > 1.4 \end{cases} \qquad \text{with} \qquad \lambda_c = \sqrt{\frac{f_y}{f_{cre}}} \quad . \quad (3)$$

where $f_{cre}$ is the minor-axis flexural buckling stress. The column ultimate strength is still determined on the basis of Eq. (1), but replacing $f_n$ by $f_{ne}$. Rasmussen (2005) followed a different path to design slender pin-ended angle columns, arguing that the angle singly-symmetry called for the consideration of an additional moment due to the effective centroid shift[9]. Quantifying this additional moment required (i) calculating an angle cross-section "effective modulus" for minor-axis bending and (ii) using an N-M interaction formula – but the extra work paid off, since this approach was shown to yield more accurate ultimate strength estimates than its predecessors.

In the last decade, the Direct Strength Method (DSM) emerged as a simple and reliable approach to design cold-formed steel members, and has already been included in the most recent North American (2007) and Australian/New Zealand (2005) cold-formed steel specifications. The DSM approach is based on the Winter-type local strength curve (Schafer 2008)

$$f_{nl} = \begin{cases} f_y & if \quad \lambda_l \leq 0.776 \\ f_y \left(\dfrac{f_{crl}}{f_y}\right)^{0.4} \left[1 - 0.15\left(\dfrac{f_{crl}}{f_y}\right)^{0.4}\right] & if \quad \lambda_l > 0.776 \end{cases} \qquad \text{with} \qquad \lambda_l = \sqrt{\frac{f_y}{f_{crl}}} \quad , \quad (4)$$

where $f_{crl}$ and $f_{nl}$ are the local buckling stress and strength. However, and since the column local and global failures often interact, the current DSM combines Eq. (4), for local failure, with Eq. (2), for global failure – $f_y$ is replaced by $f_{ne}$ in Eq. (4). The current DSM curve for local/global interactive collapse then reads

$$f_{nle} = \begin{cases} f_{ne} & if \quad \lambda_{le} \leq 0.776 \\ f_{ne} \left(\dfrac{f_{crl}}{f_{ne}}\right)^{0.4} \left[1 - 0.15\left(\dfrac{f_{crl}}{f_{ne}}\right)^{0.4}\right] & if \quad \lambda_{le} > 0.776 \end{cases} \qquad \text{with} \qquad \lambda_{le} = \sqrt{\frac{f_{ne}}{f_{crl}}} \quad , \quad (5)$$

where $f_{nle}$ is the local/global interactive strength, $f_{ne}$ is the global strength, obtained from Eq. (2), and $f_{crl}$ is the critical local buckling stress. The column ultimate load is given by

$$P_n = A \cdot f_{nle} \quad , \quad (6)$$

where $A$ is the gross cross-section area. In Eq. (1), the local and global buckling effects are dealt with separately by means of the effective area $A_e$ and global buckling strength $f_n$, respectively. Conversely, they are handled simultaneously in Eq. (6), through the local/global interactive strength $f_{nle}$.

[9] In fixed-ended columns, the effect of this effective centroid shift is fully counteracted by the presence of the minor-axis bending moment reactions.

Several cross-section geometries (*e.g.*, lipped channels, zed-sections, rack-sections or hat-sections) are currently pre-qualified for the application of the DSM. Despite their extreme geometrical simplicity, angle sections did not yet achieved such status, *i.e.*, they are not pre-qualified for the application of the current DSM design curves. Nevertheless, Rasmussen (2006) and Chodraui *et al.* (2006) proposed distinct DSM-based approaches for the design of concentrically loaded pin-ended angle columns. While the former incorporates explicitly the eccentricity due to the effective centroid shift, which amounts to treating the columns as beam-columns, the latter ignores the above eccentricity, exploring instead different relations between the local (flexural-torsional) and global (minor-axis flexural) buckling stresses. The strength curve proposed by Rasmussen (2005) reads

$$f_{nl} = \rho \cdot \beta \cdot f_y$$
$$\rho = \frac{A_e}{A} = \begin{cases} 1 & if \quad \lambda_l \le 0.673 \\ \dfrac{\lambda_l - 0.22}{\lambda_l^2} & if \quad \lambda_l > 0.673 \end{cases} \qquad \beta = \begin{cases} 1 & if \quad \lambda_l \le 1.22 \\ \dfrac{0.68}{(\lambda_l - 1)^{0.25}} & if \quad \lambda_l > 1.22 \end{cases} \tag{7}$$

and accounts simultaneously for both (i) the bending effects due to the effective centroid shift, through parameter $\beta$, and (ii) the local (torsional[10]) buckling effects, through the effective area reduction factor ρ.

Very recently, Camotim *et al.* (2012) and Silvestre *et al.* (2013) proposed different DSM-based design approaches for pin-ended and fixed-ended columns, which combine (i) the experimentally-based global strength curve proposed by Young (2004) with (ii) either the current DSM "local" strength curve, for the F columns, or an empirically modified/lowered "local" strength curve, for the P columns – the latter reads[11]

$$f_{nl} = \begin{cases} f_y & if \quad \lambda_l \le 0.71 \\ f_y \left(\dfrac{f_{crl}}{f_y}\right)\left[1 - 0.25\left(\dfrac{f_{crl}}{f_y}\right)\right] & if \quad \lambda_l > 0.71 \end{cases} \qquad \text{with} \qquad \lambda_l = \sqrt{\frac{f_y}{f_{crl}}} \ . \tag{8}$$

These DSM-based design approaches were shown (i) to provide efficient (safe, accurate and reliable[12]) estimates of the available experimental and numerical failure loads, and, moreover, (ii) to outperform their most successful predecessors, namely those proposed by Young (2004 – F columns) and Rasmussen (2006 – P columns). The experimental and numerical failure-to-predicted load ratios are given in Annexes A-D[13] – their averages, standard deviations and maximum/minimum value are summarized in Table 1. However, in spite of these rather positive performance indicators, one negative feature subsists:

[10] It is worth noting that Rasmussen (2006) based his approach on the similarity between the buckling behavior and strength of (i) angle columns (deemed to be torsional) and (ii) simply supported plate outstands (know to be local), thus disregarding the fact that short-to-intermediate angle columns buckle in a combination of torsion and major-axis flexure. Even if the flexural component is extremely minute in the shorter columns, its participation in the buckling mode becomes progressively more visible (and influential) as the column length increases – see Fig. 1(b).

[11] The designation "local" stems from the fact that the value of $f_{crl}$ appearing in Eqs. (4) and (8) corresponds, in fact, to the flexural-torsional buckling stress $f_{crft}$. Although small, the buckling mode flexural component cannot be neglected or, in other words, "local" buckling cannot be mechanically equated solely to torsional buckling (*i.e.*, the angle column behavior cannot be viewed as the "sum" of two pinned-free long plates).

[12] In particular, Camotim *et al.* (2012) and Silvestre *et al.* (2013) showed that the LRFD resistance factor $\phi$=*0.85*, employed with the current DSM, can also be adopted when applying the proposed DSM approaches for the design of angle columns.

[13] To obtain the failure load predcitions, it was necessary to calculate $f_{crft}$ and $f_{cre}$ for all the columns – their values are given in Annexes A-D. This was done by means of GBT buckling analyses carried out in the code GBTUL (Bebiano *et al.* 2008a,b).

Table 1: Means, standard deviations and maximum/minimum values of the experimental and numerical F and P column failure-to-predicted load ratios concerning the design proposals of Young (2004), Rasmussen (2006) and Silvestre *et al.* (2013)

| | F Columns | | | | P Columns | | | |
|---|---|---|---|---|---|---|---|---|
| | Young (2004) | | Silvestre *et al.* (2013) | | Rasmussen (2006) | | Silvestre *et al.* (2013) | |
| | Exp | Num* | Exp | Num | Exp | Num* | Exp | Num |
| Mean | 1.14 | 1.14 | 0.98 | 1.02 | 1.09 | 1.01 | 1.12 | 1.10 |
| Sd. Dev. | 0.18 | 0.16 | 0.15 | 0.11 | 0.24 | 0.09 | 0.25 | 0.11 |
| Max | 1.70 | 1.61 | 1.24 | 1.40 | 1.81 | 1.39 | 1.89 | 1.74 |
| Min | 0.83 | 0.95 | 0.74 | 0.73 | 0.72 | 0.81 | 0.88 | 0.96 |

(*) Values calculated for the first time in this work and concerning the column numerical analyses reported by Silvestre *et al.* (2013)

the lack of a rational structural reasoning, as reflected in (i) the almost fully empirical roots of the strength curves defined by Eqs. (3) and (8), and (ii) the inadequate nature of the only current DSM design curve involved in the approach, which predicts local failure loads (instead of flexural-torsional ones).

The following section addresses the development and assessment of novel DSM-based design approaches for F and P equal-leg short-to-intermediate angle columns, which not only (i) share (or even improve) the positive performance indicators exhibited by the approaches proposed by Camotim *et al.* (2012) and Silvestre *et al.* (2013), but also (ii) are originated by a structural reasoning closely and clearly linked to behavioral features exhibited by the angle columns (*i.e.*, deserve to be termed "rational").

## 5. Novel DSM-Based Design Approaches

As shown before, the ultimate strength of both the F and P columns is strongly affected by the "location" of the column length within the plateau, which can be quantified by either (i) the "closeness" between the $f_{crft}$ and $f_{cre}$ values or (ii) the percentage participation of major-axis flexure in the flexural-torsional buckling mode (see the $p_2$ table in Fig. 1(b)). The shorter columns, located on the left side of the plateau, exhibit (i) clearly stable post-critical behaviors, (ii) very little minor-axis flexure and (iii) very small (virtually imperceptible) $p_2$ values. Conversely, the longer columns, located on the right side of the plateau, exhibit (i) a minute/negligible post-buckling strength, (ii) considerable minor-axis flexure and (iii) visible (even if fairly small) $p_2$ values. Therefore, it may be concluded that the column failure load decreases with the length, due to a combination of (i) lower flexural-torsional post-critical strengths, "measured" by $p_2$, and (ii) higher interaction effects, "measured" by the difference between $f_{crft}$ and $f_{cre}$ – in the P columns, these interaction effects are further enhanced by the effective centroid shifts.

In order to develop rational DSM-based design approaches for F and P angle columns, it is indispensable that they reflect the behavioral features mentioned in the previous paragraph, as well as the findings of Dinis *et al.* (2012) on the mechanics of angle column instability. Therefore, it may be established, at the outset, that the sought DSM-based design approaches must exhibit the following characteristics:

(i) Since the columns fail mostly in interactive modes combining flexural (minor-axis) and flexural-torsional (major-axis) features, the strength curves involved must be ($i_1$) the current DSM global curve and ($i_2$) various flexural-torsional strength curves, specifically developed for angle columns, which replace (play the role of) the single local strength curve in the current DSM design against local-global interactive failures.

(ii) The various flexural-torsional curves must make it possible to capture the progressive erosion of the column post-critical strength as it length increases (within the $P_{cr}(L)$ curve plateau, which is obviously wider for the F columns).

(iii) The effective centroid shift effects, which strongly influence the P column ultimate strength but do not affect the F column failures, must be incorporated into the design approach through a procedure or parameter that only comes into play for the P columns, which is exactly the idea proposed by Rasmussen (2006) (see the parameter $\beta$ in Eq. (7)). However, this procedure or parameter must reflect, as closely as possible, the column flexural-torsional behavior (which varies with its length) – recall that Rasmussen based his parameter $\beta$ on local buckling concepts.

Therefore, the first step towards reaching more rational DSM design approach for angle columns consists of developing a set of genuine flexural-torsional strength curves covering adequately the whole $P_{cr}(L)$ curve plateau – naturally, these curves apply to both F and P columns, since their flexural-torsional behaviors are identical. Once this set of flexural-torsional strength curves is determined, it will be possible to propose and assess the merits of a DSM design approach for F angle columns. The same can only be achieved for P angle columns after a quantification of the effective centroid shift effects has been found. This will be done through an "amplification factor" based on the relation between the elastic behaviors of otherwise identical P and F columns (with and without effective centroid shift effects, respectively).

*5.1 Flexural-Torsional Strength Curves*

A fully numerical approach is adopted to obtain a set of "Winter-type" strength curves intended to predict, as accurately as possible, "pure flexural-torsional failures" of equal-leg angle columns buckling in flexural-torsional modes. The first step consists of determining a reasonable flexural-torsional failure load data bank, which will be then used to develop and validate the sought strength curves. This is done by determining the failure loads of *170* columns continuously restrained against minor-axis flexure, *i.e.*, "forced" to fail in a combination of major-axis flexure and torsion. The columns analyzed are all fixed-ended[14] and exhibit (i) three cross-sections (*70×1.2mm*, *50×1.2mm*, *50×2.6mm*), (ii) various lengths (all falling inside the $P_{cr}(L)$ curve plateau), (iii) critical-mode initial imperfections with amplitude equal to *L/1000* and (iv) a large number of yield stress ($f_y$) values, ranging from *30* to *2200MPa* and selected to ensure covering a wide flexural-torsional slenderness ($\lambda_{ft}$) range. Fig. 10 displays the variation of the obtained ultimate strength ratios ($f_u/f_y$) with $\lambda_{ft}$ – also depicted in this figure is the current DSM local strength curve. The observation of these results prompts the following remarks:

(i) There is no noticeable difference concerning the $f_u/f_y$ values associated with the three cross-sections considered – the corresponding "$f_u/f_y$ clouds" are virtually identical.

(ii) The huge "vertical dispersion" of the $f_u/f_y$ values makes it easy to conclude that there is no single Winter-type curve that can predict safely and accurately all of them. Moreover, it is also clear that a large number of those values fall well below the current DSM local strength curve, which means that the corresponding failure loads are considerably overestimated by this curve.

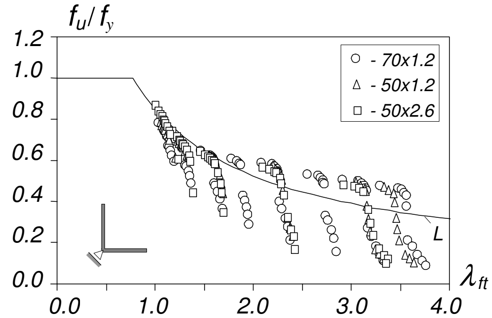


Figure 10: Variation of the column flexural-torsional ultimate strength ratios $f_u/f_y$ with $\lambda_{ft}$

[14] Recall that the pin-ended columns restrained against minor-axis flexure are a subset of their fixed-ended counterparts.

(iii) The above "vertical dispersion" is linked to the column length. Indeed, regardless of the cross-section, the $f_u/f_y$ values gradually decrease as the column length increases (along the $P_{cr}(L)$ curve plateau), which is in line with the findings reported in section 2 (for unrestrained columns).

Further investigation showed that, for any cross-section geometry, the restrained column strength (non-linear equilibrium path) consistently decreases as its length evolves along the $P_{cr}(L)$ curve plateau – Fig. 11 shows the elastic equilibrium paths of four *70×1.2mm* restrained columns with increasing lengths. Since the GBT modal participation diagrams presented in Fig. 1(b) show that the participation of major-axis flexure (mode **2**) in the column critical (flexural-torsional) buckling mode also increases with the length, it was decided to group the columns according to the ratio between their pure torsional ($f_{bt}$) and flexural-torsional ($f_{crft}$ – critical) buckling loads, which is directly linked to the participation of mode **2** – most of these two buckling loads are given in the tables presented in Annexes A-D and were calculated by means of the code GBTUL (Bebiano *et al.* 2008a,b)[15]. The $f_{bt}/f_{crft}$ ratio grows steadily as the column length increases and Figs. 12(a)-(c) show the variation of the $f_u/f_y$ with $\lambda_{ft}$ for the columns analyzed earlier that share very similar $f_{bt}/f_{crft}$ ratios – three values are considered, namely *1.0016* (Fig. 12(a)), *1.020* (Fig. 12(b)) and *1.070* (Fig. 12(c)), corresponding to column lengths located on the left side (almost pure torsional buckling), middle and right side of the $P_{cr}(L)$ curve plateau. The observation of these three figures leads to the following conclusions:

(i) Regardless of the cross-section, the $f_u/f_y$ values concerning columns sharing very similar $f_{bt}/f_{crft}$ ratios[16] are reasonably well aligned along Winter-type curves, *i.e.*, the "vertical dispersion" is fairly small.

(ii) For the columns with $f_{bt}/f_{crft}$ very close to *1* (shorter columns), the DSM local strength curve predicts reasonably well the numerical ultimate strengths. Nevertheless, it is observed that this curve provides (ii$_1$) mostly slight overestimations for $\lambda_{ft}<1.5$ and (ii$_2$) considerable underestimations for $\lambda_{ft}>1.5$ – the differences increase with the slenderness.

(iii) As $f_{bt}/f_{crft}$ increases, the DSM local strength curve predictions become progressively more unsafe in the whole slenderness range. For $f_{bt}/f_{crft}=1.070$ (longer columns), the differences are very substantial.

On the basis of the above observations, it was decided to propose a set of flexural-torsional strength curves ($f_{nft}$) exhibiting the following characteristics:

(i) Adopting "Winter-type" expressions similar to Eq. (4), which provides the current DSM local strength curve. Such expressions are of the form

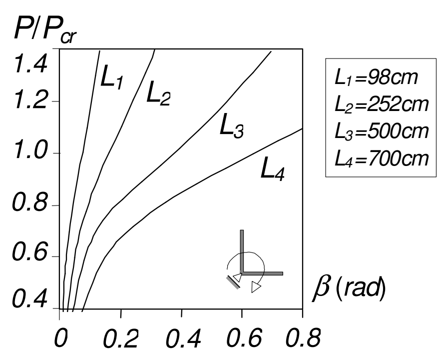


Figure 11: Equilibrium paths $P/P_{cr}$ *vs.* $\beta$ of *70×1.2mm* restrained columns with lengths $L=98; 252; 500, 700cm$

[15] The authors are currently working on the derivation of GBT-based analytical formulae to provide $f_{bt}$ and $f_{crft}$ (for angle columns).

[16] Which are assumed to exhibit also very similar post-buckling behaviors, the ratio $f_{bt}/f_{crft}$ being the key factor for this similarity.

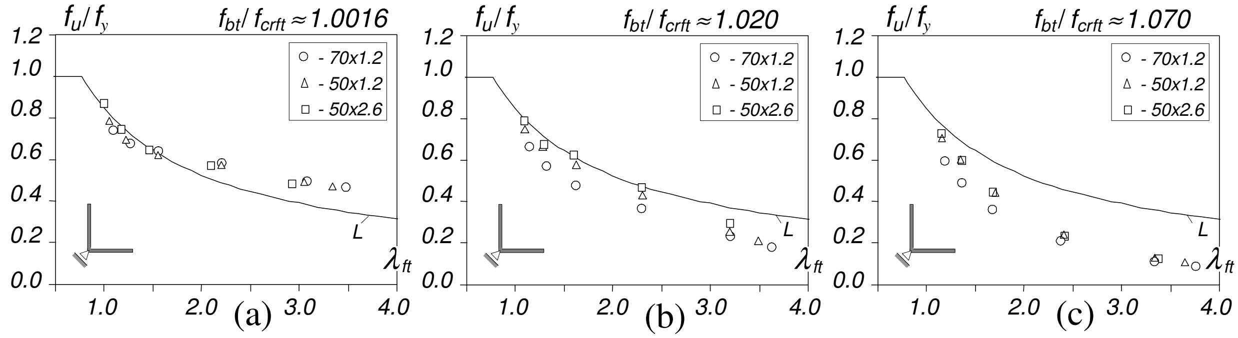


Figure 12: Variation of the $f_u/f_y$ with $\lambda_{ft}$ for $f_{bt}/f_{crft}$ values roughly equal to (a) *1.002*, (b) *1.020* and (c) *1.070*

$$f_{nft} = \begin{cases} f_y & \text{if} \quad \lambda_{ft} \le 0.641^{\frac{1}{a}} \\ f_y \left(\dfrac{f_{crft}}{f_y}\right)^a \left[1 - 0.23\left(\dfrac{f_{crft}}{f_y}\right)^a\right] & \text{if} \quad \lambda_{ft} > 0.641^{\frac{1}{a}} \end{cases} \qquad \text{with} \quad \lambda_{ft} = \sqrt{\frac{f_y}{f_{crft}}} \tag{9}$$

where parameter $a$, included to capture the strength curve dependency on the column length (within the $P_{cr}(L)$ curve plateau), is expressed in terms of the percentage ratio $\Delta_f$, which quantifies the (weakening) participation of major-axis flexure in the column critical buckling mode and is given by

$$\Delta_f = \frac{f_{bt} - f_{crft}}{f_{crft}} \times 100 \quad , \tag{10}$$

(iii) As for the expression providing the value of $a$, it was determined my means of a "trial-and-error curve-fitting procedure" based on the available numerical failure load data, concerning *170* columns continuously restrained against minor-axis flexure (see Fig. 10), assuming that $a=0.4$ corresponds to $\Delta_f=0$. The output of this effort is[17]

$$a = \begin{cases} 0.003\ \Delta_f^3 - 0.030\ \Delta_f^2 + 0.230\ \Delta_f + 0.400 & \text{if} \quad \Delta_f \le 4.0 \\ 1 & \text{if} \quad \Delta_f > 4.0 \end{cases} \quad . \tag{11}$$

Figure 13 shows a representative sample of the flexural-torsional strength curves provided by Eq. (9). They concern $\Delta_f=0.16; 1.80; 7.20$, and Fig. 13 also includes the numerical failure loads that are supposed to be predicted by these three strength curves. It is observed that:

(iii.1) The three curves follow the numerical ultimate strength trends reasonably well. Moreover, they all provide more or less accurate underestimations of the numerical failure loads.

(iii.2) For the shorter columns ($\Delta_f=0.16$), the strength curve provides rather accurate predictions, for $\lambda_{ft}<1.5$, and considerable underestimations, for higher slenderness values.

[17] At this stage, it is worth mentioning that the authors believe that it is possible to propose a more "refined" flexural-torsional strength curve set. In particular, deriving the various curves from a single expression, valid for the whole slenderness range, is not necessarily the best option. Due to time limitations, alternative flexural-torsional strength curve sets could not be duly explored up to now – this will be done shortly and the corresponding findings will be reported in the near future. Nevertheless, it should be pointed out that, as shown ahead in the paper, the proposed flexural-torsional strength curve set already leads to very good F and P angle column ultimate strength predictions – further refinements will only improve on the current status.

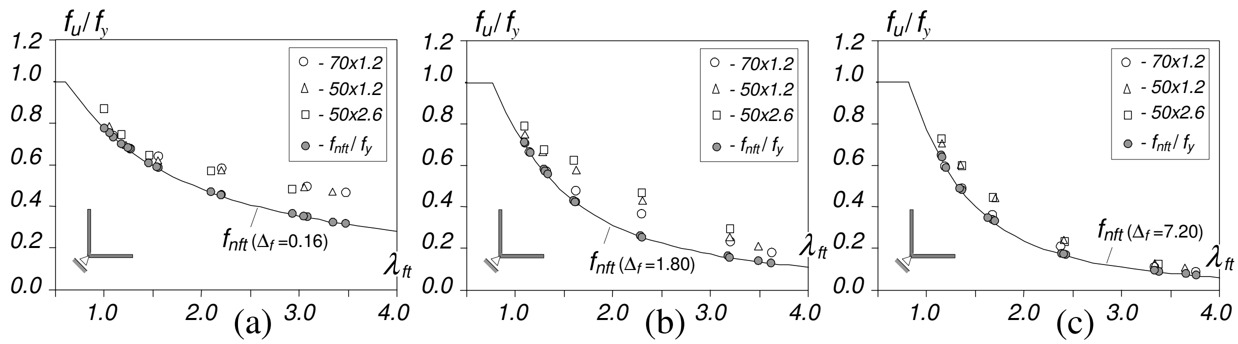


Figure 13: Proposed $f_{nft}$ strength curves for (a) $\Delta_f$=*0.16*, (b) *1.80* and (c) *7.20* and numerical failure loads predicted by them

(iii.3) For the longer columns ($\Delta_f$=*7.20*), the strength curve provides reasonable predictions for the whole slenderness range.

(iii.4) The most conservative predictions concern the intermediate columns ($\Delta_f$=*1.80*).

*5.2 DSM-Based Design Approach for Fixed-Ended Columns*

The proposed DSM-based approach to design fixed-ended equal-leg angle columns, which generally fail in flexural-torsional/flexural interactive modes, consists of combining Eq. (9) with the current DSM global strength curve, given in Eq. (2). Following the strategy adopted in the current DSM design against local-global interactive failures, $f_y$ is replaced by $f_{ne}$ in Eq. (9), leading to the to $f_{nfte}^F$ ultimate strength estimates

$$f_{nfte}^F = \begin{cases} f_{ne} & \text{if} \quad \lambda_{fte} \le 0.641^{\frac{1}{a}} \\ f_{ne}\left(\dfrac{f_{crft}}{f_{ne}}\right)^a \left[1-0.23\left(\dfrac{f_{crft}}{f_{ne}}\right)^a\right] & \text{if} \quad \lambda_{fte} > 0.641^{\frac{1}{a}} \end{cases} \qquad \text{with} \qquad \lambda_{fte} = \sqrt{\frac{f_{ne}}{f_{crft}}} \quad . \tag{12}$$

*5.3 DSM-Based Design Approach for Pin-Ended Columns*

As shown earlier, the strength differences between P and F columns stem from the effective centroid shift effects. Thus, a rational procedure must be found before it is possible to propose a DSM-based approach to design pin-ended equal-leg angle columns. The procedure adopted in this work is similar to that proposed by Rasmussen (2006), in the sense that the effective centroid shift effects are incorporated into the design approach trough a multiplicative parameter $\beta$ that depends also on the column slenderness – then, the column ultimate strength is obtained by multiplying the F column ultimate strength prediction ($f_{nfte}^F$) by the parameter $\beta$, *i.e.*,

$$f_{nfte}^P = \beta \cdot f_{nfte}^F \quad . \tag{13}$$

The procedure adopted to search for an expression providing the parameter $\beta$ is based on an "elastic reduction factor" concept that accounts for the fact that both the post-buckling strength and the effective centroid shift effects vary substantially with the column length – naturally, attention is restricted to short-to-intermediate lengths, *i.e.*, those corresponding to the P column $P_{cr}(L)$ curve plateau. This procedure involves the following steps:

(i) Perform elastic post-buckling analyses of geometrically identical F and P columns (sharing the same $f_{bt}/f_{crft}$ ratio and critical-mode initial geometrical imperfections with amplitude *L/1000*) and record the evolution, as the applied load P increases, of the maximum longitudinal normal stresses ($f_{max}$), occurring at the mid-span cross-section. For illustrative purposes, Fig. 14(a) displays the $P$ *vs.* $f_{max}$ curves concerning F and P columns associated with $\Delta_f=0.16$ ($f_{bt}/f_{crft}=1.0016$).

(ii) Assume that, for a given $f_{max}$, the difference between the corresponding F and P column applied load values ($P_F$ and $P_P$) stems from the effective centroid shift effects, which means that the ratio $P_P/P_F$ provides a good approximation for the parameter $\beta$ (*i.e.*, $\beta\approx P_P/P_F$)[18].

(iii) Relate $f_{max}$ with the column flexural-torsional slenderness by means of $\lambda_{ft}=(f_{max}/f_{crft})^{0.5}$, which amounts to assuming that $\beta$ corresponds to the strength reduction (due to the effective centroid shift effects) at the "limit elastic applied load". Then, it becomes possible to develop a set of $\beta(\lambda_{ft})$ curves, one for each $\Delta_f$ value, which will be incorporated in Eq. (14). For illustrative purposes, Fig. 14(b) displays the $\beta(\lambda_{ft})$ curves concerning the columns associated with $\Delta_f=0.16;0.84;2.41$. The differences between these curves clearly show that the relation $\beta(\lambda_{ft})$ varies with the angle column length – $\beta$ decreases substantially as the length increases. Fig. 14(b) also includes the $\beta(\lambda_{ft})$ curve proposed by Rasmussen (2006) and given in Eq. (7)[19] – note that this curve is well above its upper $\beta(\lambda_{ft})$ counterpart.

(iv) By means of a second "trial-and-error curve-fitting procedure", look for "Winter-type" expressions relating parameter $\beta$ with the column flexural-torsional slenderness $\lambda_{ft}$, of the form

$$\beta=(1-b)\left(\frac{1}{\lambda_{ft}^{2}}\right)^{c}\leq 1 \qquad , \qquad (14)$$

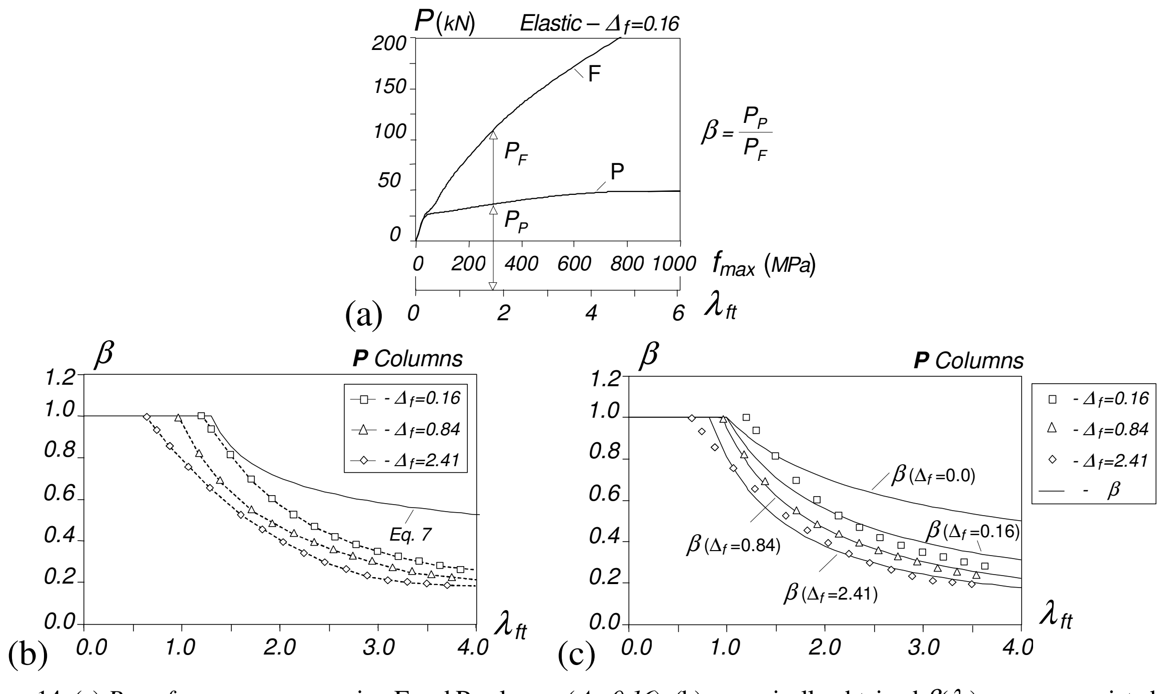


Figure 14: (a) $P$ *vs.* $f_{max}$ curves concerning F and P columns ($\Delta_f=0.16$), (b) numerically obtained $\beta(\lambda_{ft})$ curves associated with $\Delta_f=0.16;0.84;2.41$, and (c) proposed $\beta(\lambda_{ft})$ expressions for $\Delta_f=0.0;0.16;0.84;2.41$, compared with the numerical values

[18] When the P column elastic non-linear equilibrium path exhibits a limit point (this happens in a few cases – see Fig. 4), it is assumed that the corresponding $P$ *vs.* $f_{max}$ curve (see Fig 14(a)) becomes an horizontal straight line beyond that limit point – *i.e.*, the value of $P_P$ remains constant.

[19] Note that Rasmussen based his curve on local buckling concepts and, therefore, he viewed it as a $\beta(\lambda_l)$ curve.

where the dependency of $\beta$ on the column length is felt through parameters $b$ and $c$, which are expressed as functions of the percentage ratio $\Delta_f$. On the basis of the numerical results obtained, the following expressions are proposed:

$$b=\begin{cases} 0 & if \quad \Delta_f \le 0.3 \\ 0.091\ \Delta_f - 0.027 & if \quad 0.3<\Delta_f<2.5 \\ 0.2 & if \quad \Delta_f \ge 2.5 \end{cases} \tag{15}$$

$$c=\begin{cases} 0.833\ \Delta_f + 0.25 & if \quad \Delta_f < 0.3 \\ -0.009\ \Delta_f^2 + 0.047\ \Delta_f + 0.487 & if \quad 0.3 \le \Delta_f < 2.5 \\ 0.55 & if \quad \Delta_f \ge 2.5 \end{cases} \quad . \tag{16}$$

Fig. 14(c) displays (i) the $\beta$ *vs.* $\lambda_{ft}$ curves provided by Eqs. (14)-(16) for columns exhibiting $\Delta_f$=*0.0*;*0.16*;*0.84*;*2.41*, and (ii) the corresponding numerical $\beta$ values (for $\Delta_f \neq 0.0$). It is observed that the curves follow reasonably well the "exact result trends", even if there are visible differences – the most relevant occur for the shorter columns ($\Delta_f$=*0.16*). Finally, note that, since $\beta$ is used to lower the interactive strength $f_{nfte}^F$, it is just logical to express Eq. (14) in terms of the "interactive slenderness" $\lambda_{fte}$, instead of its flexural-torsional counterpart $\lambda_{ft}$.

### *5.4 Summary of the Proposed DSM Design Approaches*

The proposed DSM-based approaches for the design of fixed-ended and pin-ended equal-leg angle columns can be cast in a unified form, by means of the expressions

$$f_{nfte}=\begin{cases} \beta \cdot f_{ne} & if \quad \lambda_{fte} \le 0.641^{\frac{1}{a}} \\ \beta \cdot f_{ne} \left(\dfrac{f_{crft}}{f_{ne}}\right)^{a} \left[1-0.23\left(\dfrac{f_{crft}}{f_{ne}}\right)^{a}\right] & if \quad \lambda_{fte} > 0.641^{\frac{1}{a}} \end{cases} \quad \text{with} \quad \lambda_{fte}=\sqrt{\frac{f_{ne}}{f_{crft}}} \tag{17}$$

$$a=\begin{cases} 0.003\ \Delta_f^3 - 0.030\ \Delta_f^2 + 0.230\ \Delta_f + 0.400 & if \quad \Delta_f \le 4.0 \\ 1 & if \quad \Delta_f > 4.0 \end{cases} \tag{18}$$

$$\beta=\begin{cases} 1 & \textit{for F columns} \\ (1-b)\left(\dfrac{1}{\lambda_{ft}^2}\right)^{c} \le 1 & \textit{for P columns} \end{cases} \tag{19}$$

$$b=\begin{cases} 0 & if \quad \Delta_f \le 0.3 \\ 0.091\ \Delta_f - 0.027 & if \quad 0.3<\Delta_f<2.5 \\ 0.2 & if \quad \Delta_f \ge 2.5 \end{cases} \tag{20}$$

$$c=\begin{cases} 0.833\ \Delta_f + 0.25 & if \quad \Delta_f < 0.3 \\ -0.009\ \Delta_f^2 + 0.047\ \Delta_f + 0.487 & if \quad 0.3 \le \Delta_f < 2.5 \\ 0.55 & if \quad \Delta_f \ge 2.5 \end{cases} \quad , \tag{21}$$

where it is recalled that $\Delta_f=[(f_{bt}-f_{crft})/f_{crft}]\times 100$.

*5.5 Assessment of the Proposed DSM Design Approaches*

Attention is now turned to assessing the performance of the proposed two DSM-based design procedures, namely the DSM-F and DSM-P approaches. Their predictions ($f_{nfte}$) for the whole set of experimental and numerical column ultimate strengths are given in the tables included in Annexes A-D, together with the corresponding failure-to-predicted strength ratios $f_u/f_{nfte}$ – while Annexes A and B concern the experimental results, Annexes A and D deal with the numerical ones. Figures 12(a)-(b) provide the variation of the failure-to-predicted strength ratio $f_u/f_{nfte}$ with $\lambda_{fte}$, for the F and P columns – the associated averages, standard deviations and maximum/minimum values are given in Table 2. The observation of the results presented in these figures and table prompt the following remarks:

(i) The DSM-F procedure leads to quite accurate predictions of the experimental and numerical ultimate strengths – the $f_u/f_{nfte}$ averages and standard deviations are ($i_1$) *1.01/0.11* (experimental), ($i_2$) *1.03/0.14* (numerical results) and ($i_3$) *1.04/0.12* (experimental + numerical).

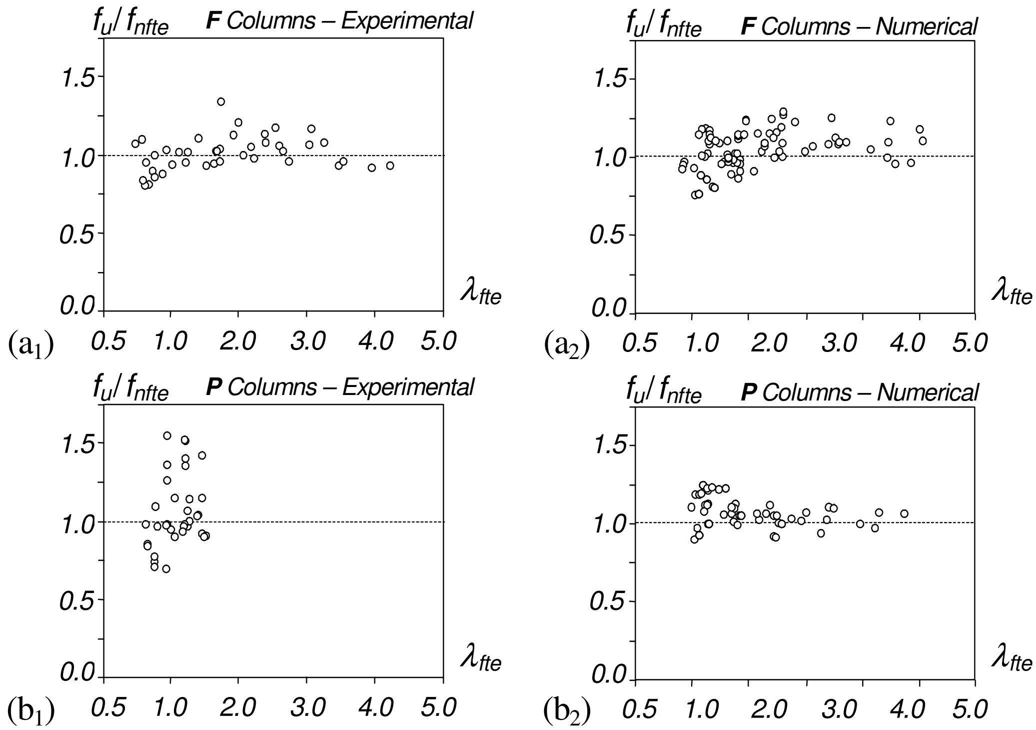


Figure 12: Variation of $f_u/f_{nfte}$ with $\lambda_{fte}$ for the (a) F and (b) P columns: ($_1$) experimental and ($_2$) numerical results

Table 2: Means, standard deviations and maximum/minimum values of the failure-to-predicted strength ratios provided by the proposed DSM design approaches for the F and P column experimental, numerical and "experimental + numerical" results

| | DSM-F approach | | | DSM-P approach | | |
|---|---|---|---|---|---|---|
| | Exp. | Num | Exp+Num | Exp | Num | Exp+Num |
| Mean | 1.01 (1.03) | 1.03 (1.04) | 1.02 (1.04) | 1.08 (1.12) | 1.07 | 1.06 (1.08) |
| Sd. Dev. | 0.11 (0.10) | 0.14 (0.12) | 0.13 (0.12) | 0.24 (0.22) | 0.10 | 0.16 (0.15) |
| Max | 1.34 (1.34) | 1.30 (1.30) | 1.34 (1.34) | 1.55 (1.55) | 1.24 | 1.55 (1.55) |
| Min | 0.80 (0.87) | 0.75 (0.80) | 0.75 (0.80) | 0.71 (0.84) | 0.90 | 0.71 (0.84) |

(ii) The DSM-P procedure also leads to very good estimates of the experimental and numerical ultimate strengths – the $f_u/f_{nfte}$ averages and standard deviations are now (ii$_1$) *1.06/0.23* (experimental), (ii$_2$) *1.07/0.10* (numerical results) and (ii$_3$) *1.06/0.16* (experimental + numerical).

(iii) The quality of the above performance indicators (iii$_1$) provides solid evidence concerning the adequacy of the reasoning behind the development of the flexural-torsional strength (F and P columns) and $\beta$ *vs.* $\lambda_{fte}$ (P columns) curves, and (iii$_2$) also indicates that the outputs of these curves reflect quite accurately the underlying structural concepts.

(iv) Nevertheless, it is worth noting that the vast majority of the unsafe strength predictions (including the most unsafe ones) concern the longer columns that exhibit very close flexural-torsional ($f_{crft}$) and flexural ($f_{cre}$) critical stresses – all differences below *1.3%* and, in a few case, even $f_{cre}<f_{crft}$. This fact raises some suspicion concerning the accuracy of the flexural-torsional strength curves associated with the higher $\Delta_f$ values, which will be further investigated in the near future[20]. Just to provide an idea of the overall benefits of improving the above estimates, Table 2 shows, between parentheses, the performance indicators obtained by excluding the corresponding *16* (out of *232*) failure loads – *10* F column (*4* experimental and *6* numerical) and *6* P column (all experimental) values. One observes that the means and standard deviations change/improve by *1-3* percentage points and, most of all, the minimum $f_u/f_{nfte}$ values increase by between *5* and *13* percentage points.

(v) The comparison between the values presented in Tables 1 and 2[21] makes it possible to conclude that the proposed design approach has performance indicators that are only slightly better than those concerning the proposals developed by Young (2004) (F columns), Rasmussen (2006) (P columns) and Silvestre *et. al.* (2013) (F and P columns). However, it has the very important advantage of being clearly more rational, in the sense that it reflects quite closely the angle column structural behavior and, moreover, retains the involvement of the current DSM global strength curve.

(vi) Finally, just two words to mention that all available P column test results (failure loads) correspond to a fairly narrow and relatively low slenderness range, thus showing the need to obtain experimental data concerning more slender P columns (to ensure proper validation for design approaches). Moreover, unlike their numerical counterparts, the P column experimental failure loads exhibit a quite large scatter, which is primarily due to a very high sensitivity to the initial minor-axis flexural imperfection sign (Mesacasa Jr. *et al.* 2012)[22] – the most detrimental sign, *i.e.*, that reinforcing the effective centroid shift effects, was always considered when determining the numerical failure loads.

The evaluation of the LRFD (Load and Resistance Factor Design) resistance factor $\phi$ associated with the proposed DSM-based approaches is addressed next. According to the North American cold-formed steel specification (AISI 2007), $\phi$ can be calculated using the formula given in section F.1.1 of chapter F,

$$\phi = C_\phi (M_m F_m P_m)\, e^{-\beta_0\sqrt{V_M^2+V_F^2+C_P V_P^2+V_Q^2}} \qquad \text{with} \qquad C_P = \left(1+\frac{1}{n}\right)\frac{m}{m-2} \quad , \quad (22)$$

---

[20] In particular, the decision of establising a “cut-off limit” $\Delta_f$*=4.0*, beyond which one has *a=1* (*i.e.*, Eq. (9) remains unchanged) seems now a bit ill-advised. Indeed, it apparently leads to an overestimation of the flexural-torsional strengths of columns with lengths very close to (or even past) the $P_{cr}(L)$ curve plateau and, consequently, also to an overestimation of the corresponding ultimate strengths. Since such columns may still fail in interactive flexural-torsional/flexural modes (instead of flexural ones, like the slightly longer columns), they should still be well handled by the proposed DSM design procedures. This is one of the aspects that will be addressed in the context of the flexural-torsional strength curve “refinement” mentioned in footnote 17.

[21] It should be pointed out that Table 2 is based on a considerably larger numerical F and P colum failure load data bank.

[22] For instance, look at the identical test trios reported by Wilhoite *et al.* (1984): while (i) the three shorter columns had very similar ultimate strengths, (ii) the intermediate columns showed some scatter (higher and lower ultimate strengths *11.5%* apart) and (iii) the longer columns exhibited an even higher scatter (*22.5%* difference).

where (i) $C_\phi$ is a calibration coefficient ($C_\phi$=1.52 for LRFD), (ii) $M_m$=1.0 and $F_m$=1.00 are the mean values of the material and fabrication factor, respectively, (iii) $\beta_0$ is the target reliability index ($\beta_0$=2.5 for structural members in LRFD), (iv) $V_M$=0.10, $V_F$=0.05 and $V_Q$=0.21 are the coefficients of variation of the material factor, fabrication factor and load effect, respectively, and (v) $C_P$ is a correction factor that depends on the numbers of tests ($n$) and degrees of freedom ($m=n-1$). In order to evaluate $\phi$ for each proposed DSM procedure (DSM-F and DSM-P), it is necessary to calculate $P_m$ and $V_P$, which are the mean and standard deviation of the "exact"-to-predicted strength ratios $f_u/f_{nfte}$ – the "exact" $f_u$ values are either experimental, numerical or experimental and numerical.

Tables 3 and 4 show the $n$, $C_P$, $P_m$, $V_P$ and $\phi$ values obtained for the column ultimate strength predictions provided by the DSM-F and DSM-P procedures applied to the experimental, numerical and total failure data – also indicate are the values (i) obtained when the *16* failure loads mentioned in the above item (iv) are excluded (between parentheses), (ii) reported by Silvestre *et. al.* (2013) and (iii) determined with the design proposals of Young (2004) and Rasmussen (2006). It is observed that:

(i) When the whole failure load data bank is considered, the resistance factor values associated with each proposed DSM-based procedure are ($i_1$) $\phi$=0.87 (F columns) and $\phi$=0.76 (P columns), for the experimental data, ($i_2$) $\phi$=0.86 (F columns) and $\phi$=0.93 (P columns), for the numerical data, and ($i_3$) $\phi$=0.87 (F and P columns), for the experimental and numerical data. these values, which are almost perfectly in line with the recommendation of the North American specification (AISI 2007) for cold-formed steel compression members ($\phi$=0.85)[23], further improve if the aforementioned *16* failure loads are exclude: ($i_1$) $\phi$=0.90 (F columns) and $\phi$=0.81 (P columns), for the experimental data, ($i_2$) $\phi$=0.89 (F columns) and $\phi$=0.93 (P columns), for the numerical data, and ($i_3$) $\phi$=0.87 (F columns) and $\phi$=0.87 (P columns), for the experimental and numerical data.

(ii) The $\phi$ values obtained with the whole failure load data bank are very similar to those reported by Silvestre *et al.* (2013). Moreover they are slightly below and above those provided by the proposals of Young (2004), for F columns, and Rasmussen (2006), for P columns – recall that these authors only employed their proposals to estimate experimental column failure loads (all the predictions concerning numerical ultimate strengths were carried out in this work).

(iii) There is substantial and solid evidence that $\phi$=0.85 can be also recommended for cold-formed steel angle compression members designed by means of the DSM-F and DSM-P procedures[24].

Table 3: LRFD resistance factors $\phi$ calculated according to AISI (2007) – DSM-F procedure and proposals from Silvestre *et al.* (2013) and Young (2004)

| | DSM-F approach | | | Silvestre *et al.* (2013) | | | Young (2004) | | |
|---|---|---|---|---|---|---|---|---|---|
| | Exp | Num | Exp+Num | Exp | Num | Exp+Num | Exp | Num | Exp+Num |
| n | 41 | 92 | 133 | 41 | 89 | 130 | 41 | 89 | 130 |
| $C_P$ | 1.078 | 1.034 | 1.023 | 1.078 | 1.035 | 1.024 | 1.078 | 1.035 | 1.024 |
| $P_m$ | 1.007 | 1.026 | 1.020 | 0.980 | 1.023 | 1.010 | 1.135 | 1.142 | 1.139 |
| $V_P$ | 0.111 | 0.137 | 0.129 | 0.145 | 0.105 | 0.120 | 0.182 | 0.157 | 0.165 |
| $\phi$ | 0.87 | 0.86 | 0.87 | 0.81 | 0.89 | 0.87 | 0.89 | 0.93 | 0.92 |

[23] This recommendation is currently not applicable to angles (Ganesan & Moen 2012).

[24] This statement will become even stronger after the flexural-torsional curve "refinement" that the authors are planning to carry out in the near future.

Table 4: LRFD resistance factors $\phi$ calculated according to AISI (2007) – DSM-P procedure and proposals from Silvestre *et al.* (2013) and Rasmussen (2006)

| | DSM-P approach | | | Silvestre *et al.* (2013) | | | Rasmussen (2006) | | |
|---|---|---|---|---|---|---|---|---|---|
| | Exp | Num | Exp+Num | Exp | Num | Exp+Num | Exp | Num | Exp+Num |
| n | 35 | 64 | 99 | 35 | 28 | 63 | 35 | 28 | 63 |
| $C_P$ | 1.093 | 1.049 | 1.031 | 1.093 | 1.119 | 1.050 | 1.093 | 1.119 | 1.050 |
| $P_m$ | 1.077 | 1.066 | 1.070 | 1.116 | 1.103 | 1.110 | 1.089 | 1.020 | 1.058 |
| $V_P$ | 0.240 | 0.101 | 0.163 | 0.246 | 0.111 | 0.196 | 0.243 | 0.145 | 0.208 |
| $\phi$ | 0.76 | 0.93 | 0.87 | 0.78 | 0.95 | 0.85 | 0.76 | 0.84 | 0.80 |

Although this feature was already shared by the proposals developed by Young (2004) (F columns) and Silvestre *et al.* (2013) (F and P columns)[25], the structural clarity and rationality of the approaches proposed in this work is definitely a significant advantage.

## 6. Conclusion

This work dealt with the development and assessment of novel procedures for the design of fixed-ended (F) and pin-ended (P) equal-leg angle columns with short-to-intermediate lengths, *i.e.*, those buckling in flexural-torsional modes. Initially, numerical results concerning the buckling and post-buckling behavior of the above angle columns were briefly presented, (i) highlighting the main differences between the F and P column responses, and (ii) evidencing the need for specific design procedures. Then, the paper gathered a large column ultimate strength data bank that included (i) experimental values, collected from the available literature and concerning *41* fixed-ended and *35* pin-ended columns, and (ii) numerical values, obtained from ABAQUS shell finite element analyses and involving *92* fixed-ended and *64* pin-ended columns with various cross-section dimensions, lengths and yield stresses.

Next, after reviewing the most efficient available methods to estimate failure loads of short-to-intermediate angle columns, the paper presented the development of novel rational DSM-based procedures to design such members. The mechanical reasoning behind these procedures is based on the fact that (i) both the F and P columns fail in interactive modes, combining (major-axis) flexural-torsional and (minor-axis) flexural deformations, and that (ii) the above interaction is much stronger in the P columns, due to the presence of effective centroid shift effects. In order to incorporate these behavioral features in the DSM design approach, it was necessary to find efficient/accurate ways to quantify (i) the F and P column flexural-torsional strength and (ii) the P columns effective centroid shift effects. These two tasks were performed numerically and led to the development of (i) genuine flexural-torsional strength curves, intended to play the role of the local strength curve in the traditional column design against local-global interactive failure, and (ii) curves providing a parameter able to capture the ultimate strength erosion stemming from the effective centroid shifts. Since the two sets of curves were found to be quite strongly length-dependent, their definition included the percentage ratio between the column pure torsional and flexural-torsional buckling loads, which is able to capture the above length-dependency, essentially linked to the participation of the minor-axis flexural deformations in the column failure modes.

[25] The proposal of Rasmussen (2006) (P columns) exhibits slightly lower $\phi$ values.

Finally, the paper closed with the assessment of the ultimate strength predictions provided by the proposed DSM design approach, by comparing them with the assembled experimental and numerical failure load data bank – both the quality and reliability of these predictions were found to be very good and, in particular, it was shown that the LRFD resistance factor $\phi$=*0.85*, currently employed for member design, can also be safely adopted for the angle columns ultimate strength predictions provided by the proposed DSM approach. Moreover, the proposed DSM-based design procedures exhibit performance indicators that compare favorably (even if only slightly) with those concerning the proposals of Young (2004) (F columns), Rasmussen (2006) (P columns) and Silvestre *et. al.* (2013) (F and P columns) – however, it has the very important advantage of being clearly more rational, in the sense that it reflects quite closely the angle column structural behavior and, moreover, still involves the current DSM global strength curve.

It still worth noting that, as mentioned earlier, the authors are currently working on the "refinement" of the angle column flexural-torsional strength curves reported here, namely by considering the possibility of having distinct curves for the low and high slenderness ranges – if successful, this research effort should further improve the proposed DSM design approach. Moreover, it is also planned to derive analytical expressions, based on Generalized Beam Theory (GBT), to calculate angle column torsional and flexural-torsional buckling loads – they will be very useful to apply the proposed DSM-based procedures.

**Acknowledgments**

The authors gratefully acknowledge the financial support of "Fundação para a Ciência e Tecnologia" (FCT – Portugal), through the research project PTDC/ECM/108146/2008 ("Generalised Beam Theory (GBT) – Development, Application and Dissemination").

## References

AISI (American Iron and Steel Institute) (1996). *AISI Specification for the Design of Cold-Formed Steel Structural Members*, Washington DC.

AISI (American Iron and Steel Institute) (2001). *North American Specification for the Design of Cold-Formed Steel Structures* (NAS), Washington DC.

AISI (American Iron and Steel Institute) (2007). *North American Specification for the Design of Cold-Formed Steel Structural Members* (NAS), Washington DC.

AS/NZS (Standards of Australia and Standards of New Zealand) (2005). *Cold-Formed Steel Structures*, Sydney-Wellington.

Bebiano R, Silvestre N, Camotim D (2008a). "*GBTUL 1.0$\beta$ – Code for Buckling and Vibration Analysis of Thin-Walled Members*", freely available at *http://www.civil.ist.utl.pt/gbt*.

Bebiano R, Silvestre N, Camotim D (2008b). "GBTUL – a code for the buckling analysis of cold-formed steel members", *Proceedings of 19th International Specialty Conference on Recent Research and Developments in Cold-Formed Steel Design and Construction* (St. Louis, 14-15/10), R. LaBoube, W.-W. Yu (eds.), 61-79.

Camotim D, Dinis PB, Silvestre N (2012). "Behaviour and design of thin-walled angle columns: geometrical simplicity vs. structural complexity", *Proceedings of 7th International Conference on Advances in Steel Structures* (ICASS 2012 – Naning, 14-16/4), S.L. Chan, G.P. Shu (eds.), Southeast University Press (Nanjing), Nanjing, 1-13 (vol. 1).

Chodraui GMB, Shifferaw Y, Malite M, Schafer BW (2006). "Cold-formed steel angles under axial compression", *Proceedings of 18th International Specialty Conference on Cold-Formed Steel Structures* (Orlando, 26-27/10), R. LaBoube, W.W. Yu (eds.), 285-300.

Dinis PB, Camotim D (2011). "Buckling, post-buckling and strength of equal-leg angle and cruciform columns: similarities and differences", *Proceedings of 6th European Conference on Steel and Composite Structures* (EUROSTEEL 2011 – Budapest, 31/8-2/9), L. Dunai, M. Iványi, K. Jármai, N. Kovács, L.G. Vigh (eds.), ECCS (Brussels), 105-110 (vol. A).

Dinis PB, Camotim D, Silvestre N (2010a). "Post-buckling behaviour and strength of angle columns", *Proceedings of International Colloquium on Stability and Ductility of Steel Structures* (SDSS'10 Rio – Rio de Janeiro, 8-10/9), E. Batista, P. Vellasco, L. Lima (eds.), 1141-1150.

Dinis PB, Camotim D, Silvestre N (2010b). "On the local and global buckling behaviour of angle, T-section and cruciform thin-walled columns and beams", *Thin-Walled Structures*, **48**(10-11), 786-797.

Dinis PB, Camotim D, Silvestre N (2011). "On the design of steel angle columns", *Proceedings of 6th International Conference on Thin-Walled Structures* (ICTWS 2011 – Timisoara, 5-7/9), D. Dubina, V. Ungureanu (eds.), 271-279.

Dinis PB, Camotim D, Silvestre N (2012). "On the mechanics of angle column instability", *Thin-Walled Structures*, **52**(March), 80-89.

Dinis PB, Green PS, Camotim D (2013). "Numerical and experimentral investigation on the post-buckling behavior, ultimate strength and design of thin-walled cruciform steel columns", *USB Key Drive Proceedings of the SSRC Annual Stability Conference* (St. Louis, 16-20/4), 2013.

Ellobody E, Young B (2005). "Behavior of cold-formed steel plain angle columns", *Journal of Structural Engineering* (ASCE), **131**(3), 469-478.

Ganesan K, Moen CD (2012). "LRFD resistance factor for cold-formed steel compression members", *Journal of Constructional Steel Research*, **72**(May), 261-266.

Kitipornchai S, Chan SL (1987). "Nonlinear finite-element analysis of angle and tee beam-columns", *Journal of Structural Engineering* (ASCE), **113**(4), 721-739.

Kitipornchai S, Albermani FGA, Chan SL (1900). "Elastoplastic finite-element models for angle steel frames", *Journal of Structural Engineering* (ASCE), **116**(10), 2567-2581.

Maia WF, Neto JM, Malite M (2008). "Stability of cold-formed steel simple and lipped angles under compression", *Proceedings of 19th International Specialty Conference on Cold-Formed Steel Structures* (St. Louis, 26-27/10), R. LaBoube, W.W. Yu (eds.), 111-125.

Mesacasa Jr. EC (2012). *Structural Behavior and Design of Cold-Formed Steel Angle Columns*, M.A.Sc. Thesis in Structural Engineering, School of Engineering at São Carlos, University of S. Paulo, Brazil. (Portuguese)

Mesacasa Jr. E, Dinis PB, Camotim D, Malite M (2012). "Mode interaction in thin-walled equal-leg angle columns", *Proceedings of 6th International Conference on Coupled Instabilities in Metal Structures* (CIMS 2012 – Glasgow, 3-5/12), J. Loughlan, D. Nash, J. Rhodes (eds.), 427-434.

Mesacasa Jr. E, Dinis PB, Camotim D, Malite M (2013). "Mode interaction and imperfection-sensitivity in thin-walled equal-leg angle columns", *submitted for publication*.

Popovic D, Hancock GJ, Rasmussen KJR (1999). "Axial compression tests of cold-formed angles", *Journal of Structural Engineering* (ASCE), **125**(5), 515-523.

Popovic D, Hancock GJ, Rasmussen KJR (2001). "Compression tests on cold-formed angles loaded parallel with a leg", *Journal of Structural Engineering* (ASCE), **127**(6), 600-607.

Rasmussen KJR (2005). "Design of angle columns with locally unstable legs", *Journal of Structural Engineering* (ASCE), **131**(10), 1553-1560.

Rasmussen KJR (2006). "Design of slender angle section beam-columns by the direct strength method", *Journal of Structural Engineering* (ASCE), **132**(2), 204-211.

Schafer BW (2008). "Review: the direct strength method of cold-formed steel member design", *Journal of Constructional Steel Research*, **64**(7-8), 766-778.

Shi G, Liu Z, Chung KF (2009). "Numerical study on the local buckling of 420 MPa steel equal angle columns under axial compression", *Proceedings of 6th International Conference on Advances in Steel Structures* (ICASS'09 – Hong Kong, 16-18/12), S.L. Chan (ed.), 387-394 (vol. I).

Shifferaw Y, Schafer BW (2011). "Behavior and design of cold-formed steel lipped and plain angles", *USB Proceedings of SSRC Annual Stability Conference* (Pittsburgh, 10-14/5).

Simulia Inc. (2008). *Abaqus Standard* (vrs. 6.7-5).

Silvestre N, Dinis PB, Camotim D (2013). "Developments on the Design of Cold-Formed Steel Angles", *Journal of Structural Engineering* (ASCE), **139**(5), in press.

Stowell EZ (1951). *Compressive Strength of Flanges*, National Advisory Committee for Aeronautics (NACA), Report Nº 1029.

Wilhoite GM, Zandonini R, Zavelani A (1984). "Behaviour and strength of angles in compression: an experimental investigation", *Proceedings of ASCE Annual Convention and Structures Congress* (San Francisco, 1-3/10).

Young B (2004). "Tests and design of fixed-ended cold-formed steel plain angle columns", *Journal of Structural Engineering* (ASCE), **130**(12), 1931-1940.

Young B, Rasmussen KJR (1999). "Shift of effective centroid in channel columns", *Journal of Structural Engineering* (ASCE), **125**(5), 524-531.

# ANNEX A

Table A: Fixed-ended column experimental ultimate strengths and their estimates according to (i) the proposals of Young (2004) and Silvestre *et al.* (2013), and (ii) the developed DSM-F procedure (dimensions in *mm*, stresses in *MPa*)

| | | Buckling analysis | | | | Test | Young (2004) | Silvestre *et al.* (2013) | | Proposed DSM-F Procedure | | | |
|---|---|---|---|---|---|---|---|---|---|---|---|---|---|
| Section | L | $f_{crft}$ | $f_{cre}$ | $f_{crt}$ | $f_y$ | $f_u$ | $f_u/f_p$ | $f_{nle}$ | $f_u/f_{nle}$ | $\Delta_f$ | a | $f_{nfte}$ | $f_u/f_{nfte}$ |
| Popovic *et al.* (1999) 50x2.5 | 150 | 375.9 | 38074.4 | 377.7 | 396 | 307.9 | 1.30 | 329.3 | 0.94 | 0.28 | 0.46 | 298.9 | 1.03 |
| | 550 | 197.6 | 2832.0 | 199.1 | 396 | 225.0 | 1.01 | 249.5 | 0.90 | 0.72 | 0.54 | 221.1 | 1.02 |
| | 970 | 185.6 | 910.5 | 189.4 | 396 | 172.9 | 0.90 | 213.6 | 0.81 | 2.03 | 0.75 | 182.5 | 0.95 |
| | 1379 | 179.6 | 450.5 | 187.1 | 396 | 154.2 | 1.00 | 172.3 | 0.89 | 4.15 | 1.00 | 152.5 | 1.01 |
| | 1747 | 174.2 | 280.7 | 186.2 | 396 | 130.4 | 1.11 | 133.2 | 0.98 | 6.88 | 1.00 | 142.4 | 0.92 |
| | 2199 | 166.5 | 177.2 | 185.7 | 396 | 110.0 | 1.44 | 88.6 | 1.24 | 11.49 | 1.00 | 125.5 | 0.88 |
| | 2598 | 158.5 | 126.9 | 185.4 | 396 | 92.9 | (1.70) | 63.0 | (1.23) | 45.94 | 1.00 | 106.6 | (0.87) |
| Popovic *et al.* (1999) 50x4.0 | 150 | 960.7 | 38825.9 | 966.6 | 388 | 424.5 | 1.26 | 385.3 | 1.10 | 0.44 | 0.49 | 386.4 | 1.10 |
| | 970 | 460.4 | 928.5 | 484.9 | 388 | 314.5 | 1.19 | 286.2 | 1.10 | 5.30 | 1.00 | 310.7 | 1.01 |
| | 1381 | 429.7 | 458.1 | 478.9 | 388 | 249.7 | 1.33 | 215.7 | 1.16 | 11.43 | 1.00 | 273.7 | 0.91 |
| | 1743 | 398.2 | 287.5 | 476.7 | 388 | 177.9 | (1.41) | 152.0) | (1.16) | 65.29 | 1.00 | 220.6 | (0.81) |
| Popovic *et al.* (1999) 50x5.0 | 150 | 1431.2 | 37819.0 | 1441.7 | 388 | 414.0 | 1.15 | 385.3 | 1.07 | 0.54 | 0.51 | 386.3 | 1.07 |
| | 970 | 667.1 | 904.4 | 723.4 | 388 | 306.8 | 1.20 | 288.2 | 1.06 | 8.42 | 1.00 | 324.2 | 0.95 |
| | 1378 | 601.6 | 448.1 | 714.5 | 388 | 216.4 | (1.21) | 213.0 | (1.02) | 58.74 | 1.00 | 270.1 | (0.80) |
| | 1749 | 531.2 | 278.2 | 711.2 | 388 | 180.0 | (1.56) | 148.0 | (1.22) | 153.92 | 1.00 | 216.4 | (0.83) |
| Young (2004) 70x1.2 | 250 | 37.6 | 28143.0 | 37.8 | 550 | 143.4 | 1.16 | 176.9 | 0.81 | 0.24 | 0.45 | 172.8 | 1.02 |
| | 1000 | 22.3 | 1758.9 | 22.3 | 550 | 112.7 | 1.03 | 127.8 | 0.88 | 0.33 | 0.47 | 160.4 | 1.03 |
| | 1500 | 21.7 | 781.7 | 21.8 | 550 | 91.6 | 0.99 | 107.0 | 0.86 | 0.61 | 0.52 | 143.3 | 0.96 |
| | 2000 | 21.4 | 439.7 | 21.6 | 550 | 75.9 | 1.04 | 84.1 | 0.90 | 1.04 | 0.60 | 125.5 | 1.02 |
| | 2500 | 21.3 | 281.4 | 21.5 | 550 | 69.9 | 1.28 | 61.8 | 1.13 | 2.30 | 0.78 | 94.5 | 0.93 |
| | 3000 | 21.2 | 195.4 | 21.4 | 550 | 48.2 | 1.10 | 48.7 | 0.99 | 0.21 | 0.45 | 154.2 | 0.93 |
| | 3500 | 21.1 | 143.6 | 21.4 | 550 | 34.9 | 0.96 | 39.9 | 0.87 | 0.13 | 0.43 | 121.0 | 0.93 |
| Young (2004) 70x1.5 | 250 | 61.8 | 27851.7 | 62.3 | 530 | 188.6 | 1.26 | 208.4 | 0.90 | 0.28 | 0.46 | 100.1 | 0.91 |
| | 1000 | 36.6 | 1740.7 | 36.9 | 530 | 147.6 | 1.12 | 151.3 | 0.98 | 0.47 | 0.50 | 79.4 | 0.96 |
| | 1500 | 35.6 | 773.7 | 36.0 | 530 | 120.0 | 1.07 | 127.0 | 0.94 | 0.75 | 0.55 | 59.9 | 1.17 |
| | 2000 | 35.2 | 435.2 | 35.6 | 530 | 83.3 | 0.93 | 100.3 | 0.83 | 1.04 | 0.60 | 45.7 | 1.05 |
| | 2500 | 34.9 | 278.5 | 35.5 | 530 | 74.8 | 1.13 | 74.0 | 1.01 | 1.42 | 0.66 | 35.9 | 0.97 |
| | 3000 | 35.6 | 193.4 | 35.4 | 530 | 62.4 | 1.17 | 58.3 | 1.07 | 0.21 | 0.44 | 184.9 | 1.02 |
| | 3500 | 34.4 | 142.1 | 35.4 | 530 | 54.8 | 1.24 | 47.2 | 1.16 | 0.24 | 0.45 | 136.9 | 1.08 |
| Young (2004) | 250 | 96.7 | 28379.0 | 97.1 | 500 | 212.4 | 1.22 | 237.2 | 0.90 | 0.45 | 0.49 | 112.7 | 1.06 |
| | 1000 | 57.0 | 1773.7 | 57.2 | 500 | 179.7 | 1.15 | 173.9 | 1.03 | 0.79 | 0.56 | 87.1 | 0.96 |
| | 1500 | 55.4 | 788.3 | 55.7 | 500 | 133.8 | 1.00 | 147.5 | 0.91 | 1.23 | 0.63 | 66.2 | 1.13 |
| | 2000 | 54.6 | 443.4 | 55.2 | 500 | 101.9 | 0.94 | 118.1 | 0.86 | 1.75 | 0.71 | 51.8 | 1.21 |
| | 2500 | 54.0 | 283.8 | 55.0 | 500 | 84.2 | 1.03 | 88.8 | 0.95 | 2.40 | 0.80 | 41.0 | 1.34 |
| | 3000 | 53.4 | 197.1 | 54.9 | 500 | 55.6 | 0.87 | 68.1 | 0.82 | 0.22 | 0.45 | 212.7 | 1.00 |
| | 3500 | 52.8 | 144.8 | 54.8 | 500 | 54.1 | 1.03 | 55.4 | 0.98 | 0.35 | 0.47 | 153.4 | 1.17 |
| Mesacasa Jr. (2011) 60x2.0 | 400 | 103.3 | 7411.3 | 103.6 | 350 | 177.1 | 1.16 | 191.0 | 0.93 | 0.69 | 0.54 | 124.4 | 1.08 |
| | 600 | 93.2 | 3293.9 | 93.6 | 350 | 166.0 | 1.11 | 179.3 | 0.93 | 1.19 | 0.62 | 96.9 | 1.05 |
| | 900 | 88.5 | 1464.0 | 89.1 | 350 | 137.0 | 0.97 | 165.9 | 0.83 | 1.87 | 0.73 | 74.8 | 1.13 |
| | 1200 | 86.6 | 823.5 | 87.5 | 350 | 128.1 | 0.97 | 151.6 | 0.85 | 2.72 | 0.84 | 59.1 | 0.94 |
| | 1800 | 84.5 | 366.0 | 86.4 | 350 | 88.0 | 0.83 | 118.4 | 0.74 | 3.77 | 0.96 | 49.1 | 1.10 |
| | | | | | | Mean | 1.14 (1.10) | Mean | 0.98 (0.95) | | | Mean | 1.01 (1.03) |
| | | | | | | Sd. Dev. | 0.18 (0.14) | Sd. Dev. | 0.15 (0.12) | | | Sd. Dev. | 0.11 (0.10) |
| | | | | | | Max. | 1.70 (1.44) | Max | 1.24 (1.24) | | | Max. | 1.34 (1.34) |
| | | | | | | Min. | 0.83 (0.83) | Min | 0.74 (0.74) | | | Min. | 0.80 (0.88) |

# ANNEX B

Table B: Pin-ended column experimental ultimate strengths and their estimates according to (i) the proposals of Rasmussen (2006) and Silvestre *et al.* (2013), and (ii) the developed DSM-P procedure (dimensions in *mm*, stresses in *MPa*)

| | | Buckling analysis | | | | Test | Rasmussen (2006) | Silvestre *et al.* (2013) | | Proposed DSM-P Procedure | | | | | | |
|---|---|---|---|---|---|---|---|---|---|---|---|---|---|---|---|---|
| Section | L | $f_{crft}$ | $f_{cre}$ | $f_{crt}$ | $f_y$ | $f_u$ | $f_u/f_p$ | $f_{nle}$ | $f_u/f_{nle}$ | $\Delta_f$ | a | b | c | β | $f_{nfte}$ | $f_u/f_{nfte}$ |
| | 823 | 156.4 | 595.7 | 157.5 | 465 | 174.3 | 1.18 | 133.8 | 1.30 | 0.70 | 0.54 | 0.04 | 0.52 | 0.65 | 122.3 | 1.42 |
| | 823 | 156.4 | 595.7 | 157.5 | 465 | 174.3 | 1.18 | 133.8 | 1.30 | 0.70 | 0.54 | 0.04 | 0.52 | 0.65 | 122.3 | 1.42 |
| Wilhoite *et al.* (1984) | 1227 | 150.0 | 268.0 | 152.1 | 465 | 140.1 | 1.27 | 109.7 | 1.28 | 1.40 | 0.66 | 0.10 | 0.54 | 0.72 | 102.8 | 1.36 |
| | 1227 | 150.0 | 268.0 | 152.1 | 465 | 144.5 | 1.30 | 109.7 | 1.32 | 1.40 | 0.66 | 0.10 | 0.54 | 0.72 | 102.8 | 1.41 |
| | 1227 | 150.0 | 268.0 | 152.1 | 465 | 156.3 | 1.41 | 109.7 | 1.42 | 1.40 | 0.66 | 0.10 | 0.54 | 0.72 | 102.8 | 1.52 |
| 70x3.0 | 1636 | 146.6 | 150.8 | 150.2 | 465 | 116.3 | 1.48 | 75.4 | 1.54 | 2.46 | 0.80 | 0.20 | 0.55 | 0.85 | 91.6 | 1.27 |
| | 1636 | 146.6 | 150.8 | 150.2 | 465 | 125.2 | 1.59 | 75.4 | 1.66 | 2.46 | 0.80 | 0.20 | 0.55 | 0.85 | 91.6 | 1.37 |
| | 1636 | 146.6 | 150.8 | 150.2 | 465 | 142.3 | 1.81 | 75.4 | 1.89 | 2.46 | 0.80 | 0.20 | 0.55 | 0.85 | 91.6 | 1.55 |
| | 286 | 237.0 | 2618.3 | 238.2 | 396 | 187.0 | 1.06 | 197.6 | 0.95 | 0.51 | 0.50 | 0.00 | 0.50 | 0.79 | 192.4 | 0.97 |
| | 285 | 237.4 | 2636.7 | 237.8 | 396 | 211.7 | 1.07 | 197.9 | 1.07 | 0.17 | 0.44 | 0.00 | 0.50 | 0.80 | 197.2 | 1.07 |
| | 490 | 201.6 | 892.0 | 202.9 | 396 | 157.8 | 1.07 | 166.7 | 0.95 | 0.64 | 0.53 | 0.03 | 0.51 | 0.75 | 157.2 | 1.00 |
| Popovic *et al.* (1999) | 490 | 201.6 | 892.0 | 202.9 | 396 | 179.8 | 1.03 | 166.7 | 1.08 | 0.64 | 0.53 | 0.03 | 0.51 | 0.75 | 157.2 | 1.14 |
| | 674 | 192.4 | 471.4 | 194.3 | 396 | 138.6 | 1.13 | 150.6 | 0.92 | 0.99 | 0.59 | 0.06 | 0.52 | 0.77 | 140.8 | 0.98 |
| | 675 | 192.3 | 470.1 | 194.3 | 396 | 213.0 | 1.42 | 150.4 | 1.42 | 1.04 | 0.60 | 0.07 | 0.53 | 0.77 | 139.6 | 1.53 |
| 50x2.5 | 900 | 186.9 | 264.4 | 190.1 | 396 | 112.6 | 1.19 | 124.6 | 0.90 | 1.71 | 0.70 | 0.13 | 0.54 | 0.81 | 124.6 | 0.90 |
| | 900 | 186.9 | 264.4 | 190.1 | 396 | 143.9 | 1.21 | 124.6 | 1.16 | 1.71 | 0.70 | 0.13 | 0.54 | 0.81 | 124.6 | 1.16 |
| | 1099 | 177.2 | 177.3 | 188.4 | 396 | 79.4 | (1.06) | 89.0 | (0.89) | 6.32 | 1.00 | 0.20 | 0.55 | 0.86 | 112.4 | (0.71) |
| | 1100 | 176.9 | 177.0 | 188.4 | 396 | 110.8 | (1.14) | 88.0 | (1.11) | 6.50 | 1.00 | 0.20 | 0.55 | 0.86 | 112.2 | (0.99) |
| Popovic *et al.* (1999) | 285 | 605.7 | 2688.8 | 609.8 | 388 | 367.1 | 1.15 | 344.4 | 1.07 | 0.68 | 0.54 | 0.03 | 0.51 | 1.00 | 334.5 | 1.10 |
| | 490 | 512.0 | 909.6 | 519.3 | 388 | 294.9 | 1.00 | 285.0 | 1.03 | 1.43 | 0.66 | 0.10 | 0.54 | 1.00 | 302.3 | 0.98 |
| 50x4.0 | 675 | 478.2 | 479.3 | 497.4 | 388 | 205.3 | (0.78) | 88.0 | (0.93) | 4.02 | 0.99 | 0.20 | 0.55 | 1.00 | 276.5 | (0.74) |
| Popovic *et al.* (1999) | 285 | 901.0 | 2619.0 | 909.6 | 388 | 360.0 | 0.99 | 350.1 | 1.03 | 0.95 | 0.59 | 0.06 | 0.52 | 1.00 | 364.7 | 0.99 |
| | 490 | 758.3 | 886.0 | 774.7 | 388 | 277.0 | 0.86 | 286.4 | 0.97 | 2.16 | 0.77 | 0.17 | 0.55 | 1.00 | 323.0 | 0.86 |
| | 490 | 758.3 | 886.0 | 774.7 | 388 | 272.8 | 0.85 | 286.4 | 0.95 | 2.16 | 0.77 | 0.17 | 0.55 | 1.00 | 323.0 | 0.84 |
| 50x5.0 | 675 | 468.2 | 466.9 | 742.1 | 388 | 213.7 | (0.78) | 218.0 | (0.98) | 58.50 | 1.00 | 0.20 | 0.55 | 1.00 | 274.0 | (0.78) |
| | 675 | 468.2 | 466.9 | 742.1 | 388 | 195.6 | (0.85) | 218.0 | (0.89) | 58.50 | 1.00 | 0.20 | 0.55 | 1.00 | 274.0 | (0.71) |
| Chodraui *et al.* (2006) | 480 | 142.9 | 1306.7 | 143.4 | 371 | 111.9 | 0.82 | 126.1 | 0.89 | 0.35 | 0.47 | 0.00 | 0.50 | 0.65 | 122.7 | 0.91 |
| | 835 | 130.1 | 431.8 | 131.1 | 371 | 104.7 | 0.91 | 109.4 | 0.96 | 0.77 | 0.55 | 0.04 | 0.52 | 0.67 | 100.0 | 1.05 |
| | 1195 | 126.1 | 210.8 | 128.0 | 371 | 83.0 | 0.91 | 89.8 | 0.92 | 1.51 | 0.67 | 0.11 | 0.54 | 0.74 | 85.3 | 0.97 |
| 60x2.4 | 1550 | 123.7 | 125.3 | 126.8 | 371 | 75.8 | 1.14 | 62.7 | 1.21 | 2.51 | 0.81 | 0.20 | 0.55 | 0.85 | 77.1 | 0.98 |
| Maia *et al.* (2008) | 480 | 144.3 | 1319.5 | 144.8 | 357 | 111.9 | 0.82 | 126.7 | 0.88 | 0.35 | 0.47 | 0.00 | 0.50 | 0.67 | 123.4 | 0.91 |
| | 650 | 135.7 | 719.6 | 136.3 | 357 | 130.3 | 1.02 | 117.5 | 1.11 | 0.44 | 0.49 | 0.01 | 0.51 | 0.67 | 112.9 | 1.15 |
| | 835 | 131.4 | 436.0 | 132.4 | 357 | 104.7 | 0.91 | 110.1 | 0.95 | 0.76 | 0.55 | 0.04 | 0.52 | 0.68 | 101.0 | 1.04 |
| 60x2.4 | 1195 | 127.3 | 212.9 | 129.2 | 357 | 81.2 | 0.88 | 91.0 | 0.89 | 1.49 | 0.67 | 0.11 | 0.54 | 0.75 | 86.4 | 0.94 |
| | 1450 | 125.5 | 144.6 | 128.3 | 357 | 75.8 | 1.02 | 71.0 | 1.07 | 2.23 | 0.77 | 0.18 | 0.55 | 0.82 | 79.5 | 0.95 |
| | | | | | | Mean | 1.09 (1.12) | Mean | 1.14 (1.14) | | | | | | Mean | 1.08 (1.12) |
| | | | | | | Sd. Dev. | 0.24 (0.24) | Sd. Dev. | 0.25 (0.25) | | | | | | Sd. Dev. | 0.24 (0.22) |
| | | | | | | Max. | 1.81 (1.81) | Max | 1.89 (1.89) | | | | | | Max. | 1.54 (1.55) |
| | | | | | | Min. | 0.72 (0.82) | Min | 0.88 (0.88) | | | | | | Min. | 0.71 (0.84) |

# ANNEX C

Table C: Fixed-ended column numerical ultimate strengths and their estimates according to (i) the proposal of Silvestre *et al.* (2013), and (ii) the developed DSM-F procedure (dimensions in *mm*, stresses in *MPa*)

| | | Buckling analysis | | | | Numerical | Silvestre *et al.* (2013) | | Proposed DSM-F Procedure | | | |
|---|---|---|---|---|---|---|---|---|---|---|---|---|
| Section | L | $f_{crft}$ | $f_{cre}$ | $f_{crt}$ | $f_y$ | $f_u$ | $f_{nle}$ | $f_u/f_{nle}$ | $\Delta_f$ | a | $f_{nfte}$ | $f_u/f_{nfte}$ |
| 70x1.2 | 532 | 27.6 | 5983.7 | 27.6 | 30 | 26.6 | 24.7 | 1.08 | 0.15 | 0.43 | 22.5 | 1.18 |
| | 980 | 24.8 | 1763.4 | 24.9 | 30 | 25.4 | 23.8 | 1.07 | 0.16 | 0.43 | 21.7 | 1.17 |
| | 1330 | 24.3 | 957.4 | 24.4 | 30 | 24.5 | 23.4 | 1.05 | 0.29 | 0.46 | 21.4 | 1.15 |
| | 1820 | 24.0 | 511.3 | 24.1 | 30 | 23.4 | 23.0 | 1.02 | 0.46 | 0.49 | 21.0 | 1.11 |
| | 2520 | 23.7 | 266.7 | 23.9 | 30 | 22.1 | 22.4 | 0.99 | 0.84 | 0.57 | 20.4 | 1.08 |
| | 3640 | 23.4 | 127.8 | 23.8 | 30 | 21.4 | 21.1 | 1.02 | 1.79 | 0.72 | 19.4 | 1.10 |
| | 4200 | 23.2 | 96.0 | 23.8 | 30 | 19.3 | 20.3 | 0.95 | 2.41 | 0.80 | 18.9 | 1.02 |
| | 5320 | 22.9 | 59.8 | 23.8 | 30 | 18.0 | 18.5 | 0.97 | 3.98 | 0.99 | 17.9 | 1.00 |
| | 7000 | 22.2 | 34.6 | 23.8 | 30 | 14.8 | 15.4 | 0.96 | 7.17 | 1.00 | 16.8 | 0.88 |
| | 8900 | 21.2 | 21.4 | 23.8 | 30 | 11.3 | 11.3 | (1.00) | 12.29 | 1.00 | 15.0 | (0.75) |
| | 532 | 27.6 | 5983.7 | 27.6 | 60 | 36.7 | 38.9 | 0.94 | 0.15 | 0.43 | 35.7 | 1.03 |
| | 980 | 24.8 | 1763.4 | 24.9 | 60 | 33.6 | 37.1 | 0.90 | 0.16 | 0.43 | 34.2 | 0.98 |
| | 1330 | 24.3 | 957.4 | 24.4 | 60 | 31.6 | 36.4 | 0.87 | 0.29 | 0.46 | 33.0 | 0.96 |
| | 1820 | 24.0 | 511.3 | 24.1 | 60 | 28.9 | 35.3 | 0.82 | 0.46 | 0.49 | 31.6 | 0.91 |
| | 2520 | 23.7 | 266.7 | 23.9 | 60 | 25.3 | 33.5 | 0.75 | 0.84 | 0.57 | 29.2 | 0.87 |
| | 3640 | 23.4 | 127.8 | 23.8 | 60 | 24.1 | 29.9 | 0.81 | 1.79 | 0.72 | 25.0 | 0.96 |
| | 4200 | 23.2 | 96.0 | 23.8 | 60 | 20.6 | 27.8 | 0.74 | 2.41 | 0.80 | 23.2 | 0.89 |
| | 5320 | 22.9 | 59.8 | 23.8 | 60 | 19.3 | 23.3 | 0.83 | 3.98 | 0.99 | 19.9 | 0.97 |
| | 7000 | 22.2 | 34.6 | 23.8 | 60 | 14.8 | 16.4 | 0.90 | 7.17 | 1.00 | 18.3 | 0.81 |
| | 8900 | 21.2 | 21.4 | 23.8 | 60 | 12.0 | 10.7 | (1.12) | 12.29 | 1.00 | 15.7 | (0.77) |
| | 532 | 27.6 | 5983.7 | 27.6 | 120 | 64.5 | 60.5 | 1.07 | 0.15 | 0.43 | 55.6 | 1.16 |
| | 980 | 24.8 | 1763.4 | 24.9 | 120 | 52.8 | 57.1 | 0.93 | 0.16 | 0.43 | 52.6 | 1.00 |
| | 1330 | 24.3 | 957.4 | 24.4 | 120 | 54.0 | 55.2 | 0.98 | 0.29 | 0.46 | 49.6 | 1.09 |
| | 1820 | 24.0 | 511.3 | 24.1 | 120 | 47.7 | 52.3 | 0.91 | 0.46 | 0.49 | 45.8 | 1.04 |
| | 2520 | 23.7 | 266.7 | 23.9 | 120 | 39.7 | 47.4 | 0.84 | 0.84 | 0.57 | 39.7 | 1.00 |
| | 3640 | 23.4 | 127.8 | 23.8 | 120 | 31.3 | 38.0 | 0.82 | 1.79 | 0.72 | 30.2 | 1.04 |
| | 4200 | 23.2 | 96.0 | 23.8 | 120 | 24.1 | 32.9 | 0.73 | 2.41 | 0.80 | 26.4 | 0.91 |
| | 5320 | 22.9 | 59.8 | 23.8 | 120 | 21.2 | 23.3 | 0.91 | 3.98 | 0.99 | 20.7 | 1.02 |
| | 7000 | 22.2 | 34.6 | 23.8 | 120 | 14.8 | 15.9 | 0.93 | 7.17 | 1.00 | 18.4 | 0.80 |
| | 8900 | 21.2 | 21.4 | 23.8 | 120 | 12.0 | 10.7 | (1.12) | 12.29 | 1.00 | 15.7 | (0.77) |
| | 532 | 27.6 | 5983.7 | 27.6 | 235 | 105.0 | 91.8 | 1.14 | 0.15 | 0.43 | 83.9 | 1.25 |
| | 980 | 24.8 | 1763.4 | 24.9 | 235 | 85.0 | 84.8 | 1.00 | 0.16 | 0.43 | 78.1 | 1.09 |
| | 1330 | 24.3 | 957.4 | 24.4 | 235 | 80.4 | 80.1 | 1.00 | 0.29 | 0.46 | 71.5 | 1.12 |
| | 1820 | 24.0 | 511.3 | 24.1 | 235 | 68.8 | 72.6 | 0.95 | 0.46 | 0.49 | 63.2 | 1.09 |
| | 2520 | 23.7 | 266.7 | 23.9 | 235 | 54.2 | 60.1 | 0.90 | 0.84 | 0.57 | 50.4 | 1.07 |
| | 3640 | 23.4 | 127.8 | 23.8 | 235 | 39.9 | 39.2 | 1.02 | 1.79 | 0.72 | 33.5 | 1.19 |
| | 4200 | 23.2 | 96.0 | 23.8 | 235 | 29.7 | 31.9 | 0.93 | 2.41 | 0.80 | 27.7 | 1.07 |
| | 5320 | 22.9 | 59.8 | 23.8 | 235 | 23.2 | 23.3 | 1.00 | 3.98 | 0.99 | 20.7 | 1.12 |
| | 7000 | 22.2 | 34.6 | 23.8 | 235 | 14.8 | 15.9 | 0.93 | 7.17 | 1.00 | 18.4 | 0.80 |
| | 8900 | 21.2 | 21.4 | 23.8 | 235 | 12.0 | 10.7 | (1.12) | 12.29 | 1.00 | 15.7 | (0.77) |
| | 532 | 27.6 | 5983.7 | 27.6 | 400 | 142.0 | 126.4 | 1.12 | 0.15 | 0.43 | 115.1 | 1.23 |
| | 980 | 24.8 | 1763.4 | 24.9 | 400 | 101.0 | 113.5 | 0.89 | 0.16 | 0.43 | 105.2 | 0.96 |
| | 1330 | 24.3 | 957.4 | 24.4 | 400 | 93.3 | 103.6 | 0.90 | 0.29 | 0.46 | 93.2 | 1.00 |
| | 1820 | 24.0 | 511.3 | 24.1 | 400 | 82.6 | 88.0 | 0.94 | 0.46 | 0.49 | 78.5 | 1.05 |
| | 2520 | 23.7 | 266.7 | 23.9 | 400 | 63.1 | 64.1 | 0.98 | 0.84 | 0.57 | 57.5 | 1.10 |
| | 3640 | 23.4 | 127.8 | 23.8 | 400 | 43.1 | 38.5 | 1.12 | 1.79 | 0.72 | 33.8 | 1.28 |
| | 4200 | 23.2 | 96.0 | 23.8 | 400 | 30.3 | 31.9 | 0.95 | 2.41 | 0.80 | 27.7 | 1.10 |

| | | Buckling analysis | | | | Numerical | Silvestre *et al.* (2013 | | Proposed DSM-F Procedure | | | |
|---|---|---|---|---|---|---|---|---|---|---|---|---|
| Section | L | $f_{crl}$ | $f_{cre}$ | $f_{crt}$ | $f_y$ | $f_u$ | $f_{nle}$ | $f_u/f_{nle}$ | $\Delta_f$ | a | $f_{nfte}$ | $f_u/f_{nfte}$ |
| | 5320 | 22.9 | 59.8 | 23.8 | 400 | 23.7 | 23.3 | 1.02 | 3.98 | 0.99 | 20.7 | 1.14 |
| | 7000 | 22.2 | 34.6 | 23.8 | 400 | 14.8 | 15.9 | 0.93 | 7.17 | 1.00 | 18.4 | 0.80 |
| | 8900 | 21.2 | 21.4 | 23.8 | 400 | 12.0 | 10.7 | (1.12) | 12.29 | 1.00 | 15.7 | (0.77) |
| | 532 | 27.6 | 5983.7 | 27.6 | 500 | 155.0 | 144.2 | 1.07 | 0.15 | 0.43 | 131.0 | 1.18 |
| | 980 | 24.8 | 1763.4 | 24.9 | 500 | 131.0 | 127.2 | 1.03 | 0.16 | 0.43 | 118.5 | 1.11 |
| | 1330 | 24.3 | 957.4 | 24.4 | 500 | 99.5 | 113.8 | 0.87 | 0.29 | 0.46 | 103.3 | 0.96 |
| 70x1.2 | 1820 | 24.0 | 511.3 | 24.1 | 500 | 93.0 | 93.0 | 1.00 | 0.46 | 0.49 | 84.7 | 1.10 |
| | 2520 | 23.7 | 266.7 | 23.9 | 500 | 65.3 | 62.7 | 1.04 | 0.84 | 0.57 | 59.3 | 1.10 |
| | 3640 | 23.4 | 127.8 | 23.8 | 500 | 43.8 | 38.5 | 1.14 | 1.79 | 0.72 | 33.8 | 1.30 |
| | 4200 | 23.2 | 96.0 | 23.8 | 500 | 30.3 | 31.9 | 0.95 | 2.41 | 0.80 | 27.7 | 1.10 |
| | 5320 | 22.9 | 59.8 | 23.8 | 500 | 23.8 | 23.3 | 1.02 | 3.98 | 0.99 | 20.7 | 1.15 |
| | 7000 | 22.2 | 34.6 | 23.8 | 500 | 14.8 | 15.9 | 0.93 | 7.17 | 1.00 | 18.4 | 0.80 |
| | 8900 | 21.2 | 21.4 | 23.8 | 500 | 12.0 | 10.7 | (1.12) | 12.29 | 1.00 | 15.7 | (0.77) |
| | 1500 | 46.5 | 384.1 | 47.0 | 120 | 52.8 | 64.0 | 0.82 | 1.18 | 0.62 | 54.5 | 0.97 |
| | 2000 | 45.8 | 216.1 | 46.8 | 120 | 46.8 | 57.1 | 0.82 | 2.12 | 0.76 | 47.4 | 0.99 |
| | 2500 | 45.2 | 138.3 | 46.7 | 120 | 42.2 | 49.3 | 0.86 | 3.34 | 0.91 | 41.4 | 1.02 |
| | 3000 | 44.5 | 96.0 | 46.7 | 120 | 36.6 | 41.1 | 0.89 | 4.92 | 1.00 | 38.1 | 0.96 |
| | 4000 | 42.7 | 54.0 | 46.6 | 120 | 29.1 | 26.6 | 1.09 | 9.21 | 1.00 | 33.8 | 0.86 |
| | 1500 | 46.5 | 384.1 | 47.0 | 235 | 80.6 | 86.4 | 0.93 | 1.18 | 0.62 | 70.1 | 1.15 |
| | 2000 | 45.8 | 216.1 | 46.8 | 235 | 63.6 | 69.6 | 0.91 | 2.12 | 0.76 | 55.1 | 1.15 |
| | 2500 | 45.2 | 138.3 | 46.7 | 235 | 50.8 | 52.5 | 0.97 | 3.34 | 0.91 | 44.3 | 1.15 |
| | 3000 | 44.5 | 96.0 | 46.7 | 235 | 38.0 | 39.8 | 0.95 | 4.92 | 1.00 | 39.1 | 0.97 |
| | 4000 | 42.7 | 54.0 | 46.6 | 235 | 29.1 | 26.6 | 1.09 | 9.21 | 1.00 | 33.8 | 0.86 |
| 50x1.2 | 1500 | 46.5 | 384.1 | 47.0 | 400 | 100.0 | 100.4 | 1.00 | 1.18 | 0.62 | 81.7 | 1.22 |
| | 2000 | 45.8 | 216.1 | 46.8 | 400 | 73.4 | 69.7 | 1.05 | 2.12 | 0.76 | 58.9 | 1.25 |
| | 2500 | 45.2 | 138.3 | 46.7 | 400 | 55.3 | 51.0 | 1.09 | 3.34 | 0.91 | 44.7 | 1.24 |
| | 3000 | 44.5 | 96.0 | 46.7 | 400 | 38.9 | 39.8 | 0.98 | 4.92 | 1.00 | 39.1 | 1.00 |
| | 4000 | 42.7 | 54.0 | 46.6 | 400 | 29.1 | 26.6 | 1.09 | 9.21 | 1.00 | 33.8 | 0.86 |
| | 1500 | 46.5 | 384.1 | 47.0 | 500 | 89.0 | 103.1 | 0.86 | 1.18 | 0.62 | 85.8 | 1.04 |
| | 2000 | 45.8 | 216.1 | 46.8 | 500 | 67.0 | 68.5 | 0.98 | 2.12 | 0.76 | 59.4 | 1.13 |
| | 2500 | 45.2 | 138.3 | 46.7 | 500 | 55.0 | 51.0 | 1.08 | 3.34 | 0.91 | 44.7 | 1.23 |
| | 3000 | 44.5 | 96.0 | 46.7 | 500 | 39.0 | 39.8 | 0.98 | 4.92 | 1.00 | 39.1 | 1.00 |
| | 4000 | 42.7 | 54.0 | 46.6 | 500 | 29.1 | 26.6 | 1.09 | 9.21 | 1.00 | 33.8 | 0.86 |
| | 950 | 219.3 | 959.9 | 224.3 | 120 | 111.0 | 110.0 | 1.01 | 2.29 | 0.78 | 113.9 | 0.97 |
| | 1500 | 208.6 | 385.0 | 220.9 | 120 | 100.0 | 96.7 | 1.03 | 5.89 | 1.00 | 105.3 | 0.95 |
| | 2000 | 197.9 | 216.6 | 219.9 | 120 | 87.8 | 81.7 | 1.07 | 11.12 | 1.00 | 95.2 | 0.92 |
| | 950 | 219.3 | 959.9 | 224.3 | 235 | 196.0 | 174.2 | 1.13 | 2.29 | 0.78 | 166.3 | 1.18 |
| | 1500 | 208.6 | 385.0 | 220.9 | 235 | 176.0 | 144.4 | 1.22 | 5.89 | 1.00 | 153.6 | 1.15 |
| 50x2.6 | 2000 | 197.9 | 216.6 | 219.9 | 235 | 128.0 | 110.8 | 1.16 | 11.12 | 1.00 | 137.5 | 0.93 |
| | 950 | 219.3 | 959.9 | 224.3 | 400 | 220.0 | 229.5 | 0.96 | 2.29 | 0.78 | 201.0 | 1.09 |
| | 1500 | 208.6 | 385.0 | 220.9 | 400 | 192.0 | 169.3 | 1.13 | 5.89 | 1.00 | 170.0 | 1.13 |
| | 2000 | 197.9 | 216.6 | 219.9 | 400 | 132.0 | 111.2 | 1.19 | 11.12 | 1.00 | 149.1 | 0.89 |
| | 950 | 219.3 | 959.9 | 224.3 | 500 | 237.0 | 253.5 | 0.94 | 2.29 | 0.78 | 214.3 | 1.11 |
| | 1500 | 208.6 | 385.0 | 220.9 | 500 | 193.0 | 174.3 | 1.11 | 5.89 | 1.00 | 174.2 | 1.11 |
| | 2000 | 197.9 | 216.6 | 219.9 | 500 | 152.0 | 108.3 | 1.40 | 11.12 | 1.00 | 150.5 | 1.01 |
| | | | | | | | Mean | 0.99 (0.98) | | | Mean | 1.03 (1.04) |
| | | | | | | | Sd. Dev. | 0.11 (0.11) | | | Sd. Dev. | 0.14 (0.12) |
| | | | | | | | Max. | 1.40 (1.40) | | | Max. | 1.34 (1.34) |
| | | | | | | | Min. | 0.73 (0.73) | | | Min. | 0.75 (0.80) |

# ANNEX D

Table D: Pin-ended column numerical ultimate strengths and their estimates according to (i) the proposal of Silvestre *et al.* (2013), and (ii) the developed DSM-P procedure (dimensions in *mm*, stresses in *MPa*)

| | | Buckling analysis | | | | Numerical | Silvestre *et al.* (2013) | | Proposed DSM-P Procedure | | | | | | |
|---|---|---|---|---|---|---|---|---|---|---|---|---|---|---|---|
| Section | L | $f_{crl}$ | $f_{cre}$ | $f_{crt}$ | $f_y$ | $f_u$ | $f_{nle}$ | $f_u/f_{nle}$ | $\Delta_f$ | a | b | c | β | $f_{nfte}$ | $f_u/f_{nfte}$ |
| 70x1.2 | 532 | 27.6 | 1495.6 | 27.6 | 30 | 24.2 | 21.1 | 1.14 | 0.15 | 0.43 | 0.00 | 0.37 | 0.97 | 21.8 | 1.11 |
| | 980 | 24.8 | 440.8 | 24.9 | 30 | 22.6 | 19.4 | 1.16 | 0.16 | 0.43 | 0.00 | 0.38 | 0.94 | 20.1 | 1.13 |
| | 1330 | 24.3 | 239.3 | 24.4 | 30 | 23.3 | 18.9 | 1.23 | 0.29 | 0.46 | 0.00 | 0.49 | 0.93 | 19.2 | 1.21 |
| | 1820 | 24.0 | 127.8 | 24.1 | 30 | 20.7 | 18.3 | 1.13 | 0.46 | 0.49 | 0.01 | 0.51 | 0.92 | 18.5 | 1.12 |
| | 2520 | 23.7 | 66.7 | 23.9 | 30 | 18.7 | 17.3 | 1.08 | 0.84 | 0.57 | 0.05 | 0.52 | 0.93 | 17.4 | 1.07 |
| | 3640 | 23.4 | 32.0 | 23.8 | 30 | 15.1 | 14.7 | 1.03 | 1.79 | 0.72 | 0.14 | 0.54 | 0.93 | 15.6 | 0.97 |
| | 4200 | 23.2 | 24.0 | 23.8 | 30 | 13.2 | 12.6 | 1.05 | 2.41 | 0.80 | 0.19 | 0.55 | 0.94 | 14.7 | 0.90 |
| | 532 | 27.6 | 1495.6 | 27.6 | 60 | 26.9 | 24.3 | 1.11 | 0.15 | 0.43 | 0.00 | 0.37 | 0.75 | 26.7 | 1.01 |
| | 980 | 24.8 | 440.8 | 24.9 | 60 | 24.0 | 22.0 | 1.09 | 0.16 | 0.43 | 0.00 | 0.38 | 0.73 | 24.2 | 0.99 |
| | 1330 | 24.3 | 239.3 | 24.4 | 60 | 23.9 | 21.4 | 1.12 | 0.29 | 0.46 | 0.00 | 0.49 | 0.68 | 21.2 | 1.13 |
| | 1820 | 24.0 | 127.8 | 24.1 | 60 | 21.0 | 20.6 | 1.02 | 0.46 | 0.49 | 0.01 | 0.51 | 0.68 | 19.8 | 1.06 |
| | 2520 | 23.7 | 66.7 | 23.9 | 60 | 18.8 | 19.3 | 0.97 | 0.84 | 0.57 | 0.05 | 0.52 | 0.71 | 17.9 | 1.05 |
| | 3640 | 23.4 | 32.0 | 23.8 | 60 | 15.3 | 15.0 | 1.02 | 1.79 | 0.72 | 0.14 | 0.54 | 0.79 | 15.4 | 0.99 |
| | 4200 | 23.2 | 24.0 | 23.8 | 60 | 13.4 | 12.0 | 1.12 | 2.41 | 0.80 | 0.19 | 0.55 | 0.85 | 14.6 | 0.92 |
| | 532 | 27.6 | 1495.6 | 27.6 | 120 | 29.4 | 25.9 | 1.14 | 0.15 | 0.43 | 0.00 | 0.37 | 0.59 | 32.1 | 0.92 |
| | 980 | 24.8 | 440.8 | 24.9 | 120 | 25.9 | 23.3 | 1.11 | 0.16 | 0.43 | 0.00 | 0.38 | 0.57 | 28.4 | 0.91 |
| | 1330 | 24.3 | 239.3 | 24.4 | 120 | 25.5 | 22.5 | 1.13 | 0.29 | 0.46 | 0.00 | 0.49 | 0.51 | 22.8 | 1.12 |
| | 1820 | 24.0 | 127.8 | 24.1 | 120 | 21.0 | 21.7 | 0.97 | 0.46 | 0.49 | 0.01 | 0.51 | 0.53 | 20.6 | 1.02 |
| | 2520 | 23.7 | 66.7 | 23.9 | 120 | 18.8 | 19.6 | 0.96 | 0.84 | 0.57 | 0.05 | 0.52 | 0.60 | 18.0 | 1.05 |
| | 3640 | 23.4 | 32.0 | 23.8 | 120 | 15.3 | 14.8 | 1.03 | 1.79 | 0.72 | 0.14 | 0.54 | 0.78 | 15.4 | 0.99 |
| | 4200 | 23.2 | 24.0 | 23.8 | 120 | 13.4 | 12.0 | 1.12 | 2.41 | 0.80 | 0.19 | 0.55 | 0.85 | 14.6 | 0.92 |
| | 532 | 27.6 | 1495.6 | 27.6 | 235 | 38.4 | 26.7 | 1.44 | 0.15 | 0.43 | 0.00 | 0.37 | 0.46 | 37.7 | 1.02 |
| | 980 | 24.8 | 440.8 | 24.9 | 235 | 30.3 | 23.9 | 1.27 | 0.16 | 0.43 | 0.00 | 0.38 | 0.46 | 32.4 | 0.93 |
| | 1330 | 24.3 | 239.3 | 24.4 | 235 | 25.7 | 23.1 | 1.11 | 0.29 | 0.46 | 0.00 | 0.49 | 0.40 | 24.0 | 1.07 |
| | 1820 | 24.0 | 127.8 | 24.1 | 235 | 21.0 | 21.8 | 0.96 | 0.46 | 0.49 | 0.01 | 0.51 | 0.46 | 21.0 | 1.00 |
| | 2520 | 23.7 | 66.7 | 23.9 | 235 | 18.8 | 19.5 | 0.96 | 0.84 | 0.57 | 0.05 | 0.52 | 0.59 | 18.0 | 1.05 |
| | 3640 | 23.4 | 32.0 | 23.8 | 235 | 15.3 | 14.8 | 1.03 | 1.79 | 0.72 | 0.14 | 0.54 | 0.78 | 15.4 | 0.99 |
| | 4200 | 23.2 | 24.0 | 23.8 | 235 | 13.4 | 12.0 | 1.12 | 2.41 | 0.80 | 0.19 | 0.55 | 0.85 | 14.6 | 0.92 |
| | 532 | 27.6 | 1495.6 | 27.6 | 400 | 45.2 | 27.0 | 1.67 | 0.15 | 0.43 | 0.00 | 0.37 | 0.39 | 42.3 | 1.07 |
| | 980 | 24.8 | 440.8 | 24.9 | 400 | 28.2 | 24.1 | 1.17 | 0.16 | 0.43 | 0.00 | 0.38 | 0.40 | 35.3 | 0.99 |
| | 1330 | 24.3 | 239.3 | 24.4 | 400 | 27.1 | 23.1 | 1.17 | 0.29 | 0.46 | 0.00 | 0.49 | 0.36 | 24.6 | 1.10 |
| | 1820 | 24.0 | 127.8 | 24.1 | 400 | 21.0 | 21.7 | 0.97 | 0.46 | 0.49 | 0.01 | 0.51 | 0.45 | 21.0 | 1.00 |
| | 2520 | 23.7 | 66.7 | 23.9 | 400 | 18.8 | 19.5 | 0.96 | 0.84 | 0.57 | 0.05 | 0.52 | 0.59 | 18.0 | 1.05 |
| | 3640 | 23.4 | 32.0 | 23.8 | 400 | 15.3 | 14.8 | 1.03 | 1.79 | 0.72 | 0.14 | 0.54 | 0.78 | 15.4 | 0.99 |
| | 4200 | 23.2 | 24.0 | 23.8 | 400 | 13.4 | 12.0 | 1.12 | 2.41 | 0.80 | 0.19 | 0.55 | 0.85 | 14.6 | 0.92 |
| | 532 | 27.6 | 1495.6 | 27.6 | 500 | 47.1 | 27.1 | 1.74 | 0.15 | 0.43 | 0.00 | 0.37 | 0.36 | 44.2 | 1.07 |
| | 980 | 24.8 | 440.8 | 24.9 | 500 | 28.2 | 24.2 | 1.17 | 0.16 | 0.43 | 0.00 | 0.38 | 0.38 | 36.3 | 0.97 |
| | 1330 | 24.3 | 239.3 | 24.4 | 500 | 27.1 | 23.1 | 1.18 | 0.29 | 0.46 | 0.00 | 0.49 | 0.35 | 24.7 | 1.10 |
| | 1820 | 24.0 | 127.8 | 24.1 | 500 | 21.0 | 21.7 | 0.97 | 0.46 | 0.49 | 0.01 | 0.51 | 0.45 | 21.0 | 1.00 |
| | 2520 | 23.7 | 66.7 | 23.9 | 500 | 18.8 | 19.5 | 0.96 | 0.84 | 0.57 | 0.05 | 0.52 | 0.59 | 18.0 | 1.05 |
| | 3640 | 23.4 | 32.0 | 23.8 | 500 | 15.3 | 14.8 | 1.03 | 1.79 | 0.72 | 0.14 | 0.54 | 0.78 | 15.4 | 0.99 |
| | 4200 | 23.2 | 24.0 | 23.8 | 500 | 13.4 | 12.0 | 1.12 | 2.41 | 0.80 | 0.19 | 0.55 | 0.85 | 14.6 | 0.92 |
| 50x1.2 | 750 | 48.3 | 384.1 | 48.5 | 120 | 45.3 | 42.3 | 1.07 | 0.33 | 0.47 | 0.00 | 0.50 | 0.67 | 41.4 | 1.09 |
| | 950 | 47.5 | 239.4 | 47.8 | 120 | 42.7 | 40.9 | 1.05 | 0.51 | 0.50 | 0.02 | 0.51 | 0.68 | 38.8 | 1.10 |
| | 1500 | 46.5 | 96.0 | 47.0 | 120 | 40.1 | 35.8 | 1.12 | 1.18 | 0.62 | 0.08 | 0.53 | 0.73 | 33.0 | 1.22 |
| | 2000 | 45.8 | 54.0 | 46.8 | 120 | 36.5 | 26.4 | 1.38 | 2.12 | 0.76 | 0.17 | 0.55 | 0.82 | 29.4 | 1.24 |
| | 750 | 48.3 | 384.1 | 48.5 | 235 | 46.5 | 44.5 | 1.04 | 0.33 | 0.47 | 0.00 | 0.50 | 0.51 | 43.9 | 1.06 |

| | | Buckling analysis | | | | Numerical | Silvestre *et al.* (2013) | | Proposed DSM-P Procedure | | | | | | |
|---|---|---|---|---|---|---|---|---|---|---|---|---|---|---|---|
| Section | L | $f_{crl}$ | $f_{cre}$ | $f_{crt}$ | $f_y$ | $f_u$ | $f_{nle}$ | $f_u/f_{nle}$ | $\Delta_f$ | a | b | c | β | $f_{nfte}$ | $f_u/f_{nfte}$ |
| 50x1.2 | 950 | 47.5 | 239.4 | 47.8 | 235 | 42.7 | 42.8 | 1.00 | 0.51 | 0.50 | 0.02 | 0.51 | 0.54 | 40.1 | 1.06 |
| | 1500 | 46.5 | 96.0 | 47.0 | 235 | 40.1 | 35.2 | 1.14 | 1.18 | 0.62 | 0.08 | 0.53 | 0.67 | 32.8 | 1.22 |
| | 2000 | 45.8 | 54.0 | 46.8 | 235 | 36.5 | 26.4 | 1.38 | 2.12 | 0.76 | 0.17 | 0.55 | 0.82 | 29.4 | 1.24 |
| | 750 | 48.3 | 384.1 | 48.5 | 400 | 46.5 | 45.3 | 1.03 | 0.33 | 0.47 | 0.00 | 0.50 | 0.43 | 45.3 | 1.03 |
| | 950 | 47.5 | 239.4 | 47.8 | 400 | 42.7 | 43.0 | 0.99 | 0.51 | 0.50 | 0.02 | 0.51 | 0.47 | 40.7 | 1.05 |
| | 1500 | 46.5 | 96.0 | 47.0 | 400 | 40.1 | 35.2 | 1.14 | 1.18 | 0.62 | 0.08 | 0.53 | 0.67 | 32.8 | 1.22 |
| | 2000 | 45.8 | 54.0 | 46.8 | 400 | 36.5 | 26.4 | 1.38 | 2.12 | 0.76 | 0.17 | 0.55 | 0.82 | 29.4 | 1.24 |
| | 750 | 48.3 | 384.1 | 48.5 | 500 | 46.5 | 45.4 | 1.02 | 0.33 | 0.47 | 0.00 | 0.50 | 0.41 | 45.7 | 1.02 |
| | 950 | 47.5 | 239.4 | 47.8 | 500 | 42.7 | 42.8 | 1.00 | 0.51 | 0.50 | 0.02 | 0.51 | 0.46 | 40.8 | 1.05 |
| | 1500 | 46.5 | 96.0 | 47.0 | 500 | 40.1 | 35.2 | 1.14 | 1.18 | 0.62 | 0.08 | 0.53 | 0.67 | 32.8 | 1.22 |
| | 2000 | 45.8 | 54.0 | 46.8 | 500 | 36.5 | 26.4 | 1.38 | 2.12 | 0.76 | 0.17 | 0.55 | 0.82 | 29.4 | 1.24 |
| 50x2.6 | 750 | 224.5 | 385.0 | 227.8 | 235 | 182.0 | 142.6 | 1.28 | 1.45 | 0.67 | 0.11 | 0.54 | 1.00 | 153.9 | 1.18 |
| | 950 | 219.3 | 239.9 | 224.4 | 235 | 154.0 | 119.2 | 1.29 | 2.34 | 0.79 | 0.19 | 0.55 | 0.98 | 140.0 | 1.10 |
| | 750 | 224.5 | 385.0 | 227.8 | 400 | 189.0 | 159.8 | 1.18 | 1.45 | 0.67 | 0.11 | 0.54 | 0.83 | 154.3 | 1.22 |
| | 950 | 219.3 | 239.9 | 224.4 | 400 | 164.0 | 123.8 | 1.32 | 2.34 | 0.79 | 0.19 | 0.55 | 0.86 | 138.6 | 1.18 |
| | 750 | 224.5 | 385.0 | 227.8 | 500 | 189.0 | 162.5 | 1.16 | 1.45 | 0.67 | 0.11 | 0.54 | 0.78 | 153.7 | 1.23 |
| | 950 | 219.3 | 239.9 | 224.4 | 500 | 164.0 | 120.0 | 1.37 | 2.34 | 0.79 | 0.19 | 0.55 | 0.84 | 138.1 | 1.19 |
| | | | | | | | Mean | 1.14 | | | | | | Mean | 1.07 |
| | | | | | | | Sd. Dev. | 0.16 | | | | | | Sd. Dev. | 0.10 |
| | | | | | | | Max. | 1.74 | | | | | | Max. | 1.24 |
| | | | | | | | Min. | 0.96 | | | | | | Min. | 0.90 |